The formation and differentiation of magmas

Alferyeva Ya.O., Novikova A.S. Experimental study of phase relations in crystallization of ongonite melts from the Ary-Bulak intrusion

Lomonosov Moscow State University, Department of Geology, Moscow

Abstract. Samples from three several zones of Ary-Bulak 1) porphyritic ongonites, 2) high Ca and F porphyritic ongonites, and 3) aphyric rock were explored under the temperatures 700 and 800°C and pressure 1 kBar with different amount of water 3, 5 10% on hydrothermal high-pressure equipment. Liquidus is attained for high Ca and F porphyritic and aphyric ongonites. Liquidus phases for them are fluorine and topaz.

Keywords: *ongonites, high-fluoride granite systems.*

Experimental melting study of three several zones of Ary-Bulak massive were explored to define mineralogical phases and order of crystallization of rocks. They were made on Department of Experimental Petrology in Moscow State University of M. V. Lomonosov on hydrothermal high-pressure plant with external heating and cold-seal by the temperatures 700 and 800˚C and pressure 1 kBar. The accuracy of leading experimental study was 10˚C and 100 Bar. Experiments by 800°C have lasted 7 days, and by 700°C – 14 days. The duration of cooling 10 minutes.

Samples from three different zones - central zone of porphyritic ongonites (ARB-28), the intermediate zone consist of high Ca and F porphyritic ongonites (ARB-24), and the marginal zone composed of aphyric rock (ARB-19) were used as source material. All samples were given by I.S. Peretagko. More information about their petrological and mineralogical composition is in articles written by (Peretyazhko et al., 2007, 2010, 2011). Full description of geologic structure is also situated in works of (Kovalenko and others, 1976, 1999; Antipin et al., 2009).

Samples were explored by adding different amount of water, received mix was put in platinum ampule, when was sealed up from two sides. Experiments, conducted by 800°C, contained 3, 10 and 15 mass.% water, by 700°C - 10 mass.%.

Rock samples have special petrochemical aspects, which are reflected in results of experiment. In this rock series from central zone of porphyritic ongonites till marginal zone of aphyric ongonites the common trend is directed towards decreasing content of alkalies and silicium and rising content of F and Ca.

Melting products of porphyric ongonites central zone (ARB-28) by 700 and 800 °C with different amounts of water have the same composition (tab.1, picture 1,2) The result data experiments contain of aluminosilicate glass with small number of quenching phases. Glass is close to value composition of rocks. A few flakes ore minerals are close to Nb columbite.

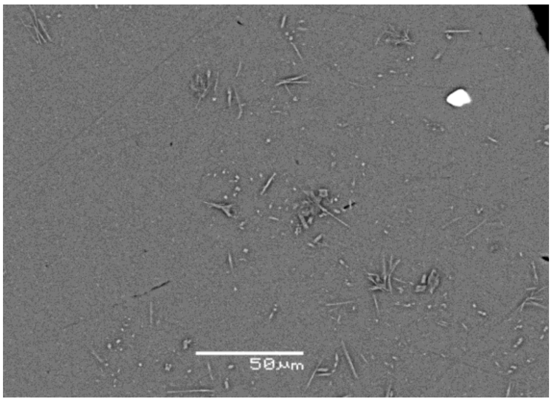

Picture 1. Porphyric ongonites of central zone (ARB-28) after the experiments at 700 and 800°C with different amount of water

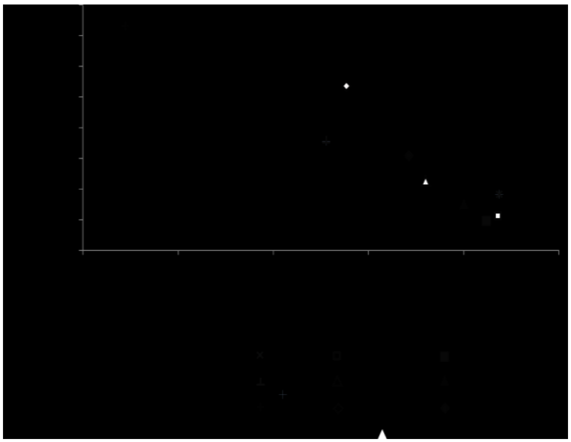

Picture 2. Changes in the SiO_2 and F content in the gross volume and the residual melt of the samples.

At 800°C Ca-F porphyritic ongonites (ARB-24) composed of aluminosilicate melt (95%) and fluorite (5%). Fluorite crystals attain a size 10 mkm (picture 3a). They frequently haven't crystalline faces and presented by rounded flakes, rising 5-7 mkm. Sometimes they form rounded agglomerates 50 mkm wide. Different amount of water within the prescribed limits doesn't influence mineralogical phases and order of crystallization of rocks.(tab.1)

On sample ARB-24 by 700˚C (picture 3b) equilibrium crystal phases, besides fluorite (15-20%) are topaz (till 5%) and plagioclase (15-20%). There is also a high quantity of melt (60-65%). The size of fluorite increase approximately till 15 mkm. There are as rounded, as crystalline faced crystals.

Plagioclase is represented by elongated subidiomorphic or skeletal crystals up to 20 microns in size. Topaz-elongated or isometric zonal crystals up to 15 microns in size. The size of fluorite flakes allows to determine its composition with sufficient accuracy (about 10 reproducible measurements in each sample) and to determine the presence of silicon impurities (0.2 at.%), aluminum (0,1 at.%), oxygen (2 at.%). The composition of the plagioclase corresponds to andesine. The ratio of atomic fluorine to oxygen in Topaz is 1:2.

Table 1. The gross composition of the source rocks and the composition of the phases the products of the experiments (mass.%). Symbols: dash - no data, L-silicate glass, Fly-fluorite, Toz-Topaz, Pl-plagioclase.

№ sample	LOI	Amount of water	Phase	SiO_2	Al_2O_3	Na_2O	K_2O	CaO	F	O=2F	Sum
Parent rock											
ARB-28	1,57	-	over all comp	71,86	16,86	3,89	4,50	0,17	1,83	0,77	99,04
ARB-24	3,92	-	over all comp	62,78	14,83	3,44	3,96	9,85	3,56	1,50	97,74
ARB-19	9,48	-	over all comp	52,23	18,64	0,46	3,11	14,79	7,31	3,08	94,06
800°C											
ARB-28	-	3	L	71,81	14,29	3,68	4,60	0,20	1,35	0,57	95,36
	-	10	L	71,36	14,14	3,46	4,66	0,17	0,74	0,31	94,23
	-	15	L	72,19	14,20	3,66	4,61	0,20	1,29	0,54	95,61
ARB-24	-	3	L	68,60	15,32	3,43	4,46	1,71	2,32	0,98	94,86
	-	10	L	66,97	15,16	3,21	4,29	1,74	2,31	0,97	92,70
	-	15	L	68,43	15,40	3,37	4,35	1,69	2,19	0,92	94,50
ARB-19	-	3	L	62,15	17,41	0,59	4,27	3,98	6,03	2,54	91,90
	-	10	L	66,42	14,44	0,61	4,37	2,61	4,09	1,72	90,83
	-	15	L	62,95	17,05	0,66	4,16	3,94	5,94	2,50	92,19
700°C											
ARB-28	-	10	L	71,18	14,49	2,76	4,60	0,22	0,96	0,40	93,82
ARB-24	-	10	L	70,01	13,91	1,59	4,32	1,56	1,52	0,64	92,27
	-	10	Pl	59,97	25,34	6,31	0,87	7,50	0,09	0,04	100,0
	-	10	Toz	32,52	56,56	0,00	0,05	0,12	18,73	7,89	100,1
ARB-19	-	10	L	67,12	15,36	0,39	4,64	3,08	3,09	1,30	92,38
	-	10	Qtz?	98,82	1,42	0,00	0,21	0,21	0,48	0,20	100,1
	-	10	Toz	36,57	51,64	0,00	0,51	0,40	18,5	7,81	99,86
	-	10	Pl	48,94	32,70	1,88	0,39	15,48	0,06	0,03	99,42

The composition of silicate melt is generally less siliceous than that of ARB-28 (Fig. 2). If possible losses of fluorine during crystallization of ongonites are neglected, then the gross composition of the sample can be considered as the melt composition of the superliquid region. Then the trend in figure 2 reflects the change in the composition of the residual melt during the crystallization of these rocks.

A system keeps the saturation condition on high fluorine phases (fluorine and topaz), while amount of F is rising and amount of Si is decreasing.

At 800°C in marginal aphyric (ARB-19) zones (pct.4a) stable melt (80-85%), fluorite (5-7%), topaz (5-10%).

Fluorite, as in porphyritic ongonites, has both faceted and rounded grains, 20 mkm at size. Topaz is represented by small (up to 5 microns) elongated crystals. Plagioclase and substantially SiO_2 phase appear when temperature decreases till 700°C. (pct.4b). Samples contain 50% glass, 15% fluorite, 15% plagioclase, 5-10% Topaz, 10% high-silicon phase. A lack of crystal outlines, the size from the first microns to the first tens of microns, the presence of silicate glass inclusions, rounded isometric and elongated forms is inherent in high-silicon phases.

Fluorite has impurities of silicium, aluminium and etc. Composition of plagioclase indicate bytownite. Ratio of F to O in topaz has an average out ½. The composition of the high-silicon phase is close to quartz, and is characterized by the presence of impurities of alumina, alkalis, fluorine. According to the size of phase and the reproducibility of analyses it is highly likely to consider impurities to be fingerprint to high-silicon phase.

Value composition and glass of ARB-19 are less siliceous than in the case of porphyry Ca-F ongonite. While temperature decreases the residual liquor enriches by Si and depletes F.

The phase relations in ongonite melt crystallization are found in accordance with previous results in modeling haplogranite high-fluoride system (Gramenitsky et al., 2005, Alferyeva et al., 2011, 2018, Shchekina et al., 2013).

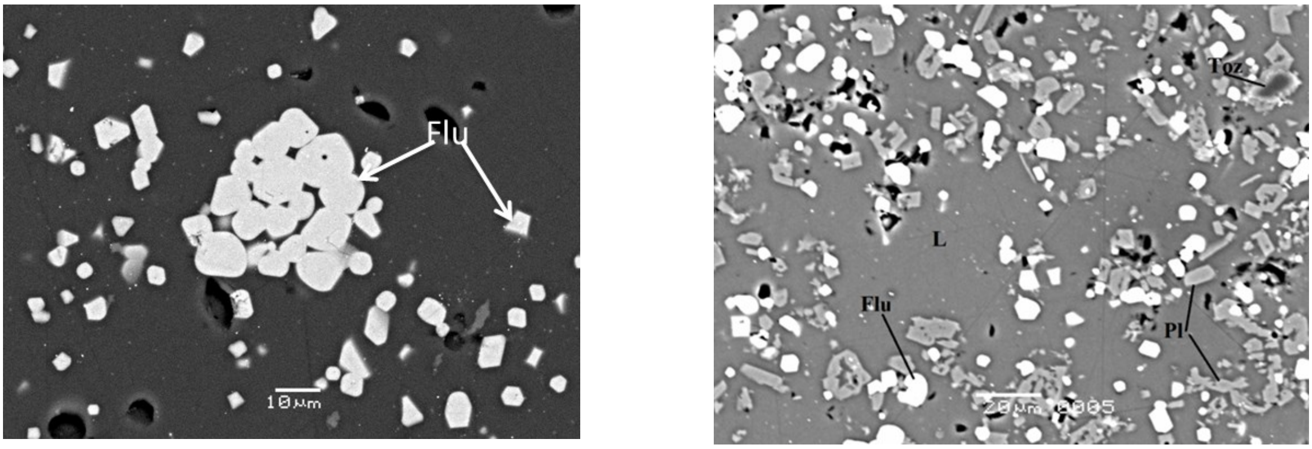

a. b.

Picture 3. Porphyryc Ca-F ongonite (ARB-24) after experiments at a) 800˚C with a different amount of water and b) 700˚C

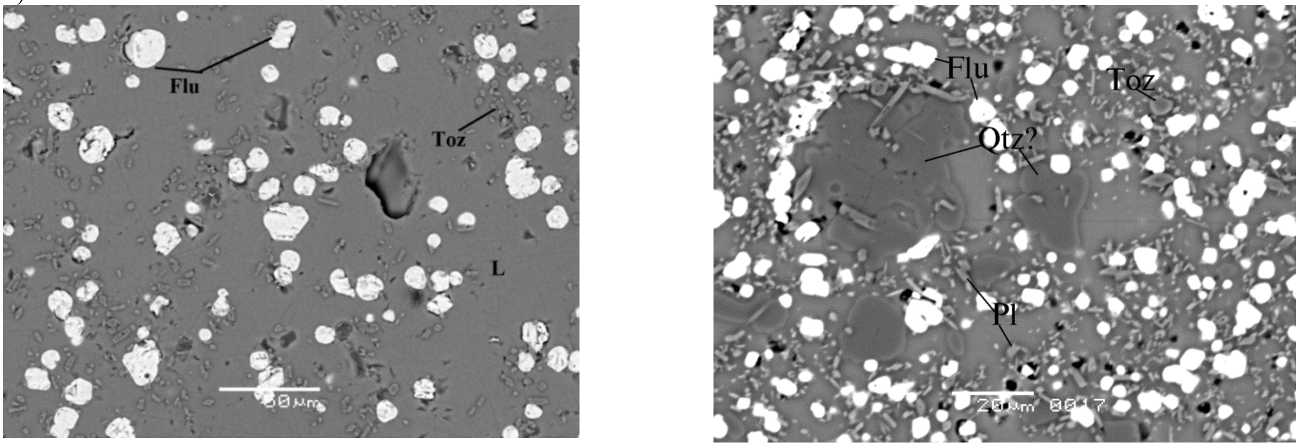

a. b.

Picture 4. Ongonit aphyric facies of endocontact (ARB-19) after the experiments at a) 800˚C with different amounts of water and b) 700˚C

Conclusions.

1. The results of the experiment have showed that different amounts of water give the same results and doesn’t influence on mineralogical phases and order of crystallization of rocks.
2. Liquidus phases for marginal zones - of Ca-F porphyritic (ARB 24) and aphyric (ARB 19) ongonites are fluorite and topaz.
3. The crystallization of central porphyric zone begins under 700°C.

References:

Alferyeva J. O., Gramenitskii E. N., Shchekina T. I. Experimental study of phase relations in a lithium-containing fluorine haplogranite and nepheline-syenite system // Geochemistry. No. 7. 2011. P. 713-728.

Alferyeva J. O., Shchekina T. I., Gramenitskii E. N., Limit the content of fluorine and water in granite melts highly evolved // Vestn. Mosk. Un. Ser. 4. Geology. 2018. No. 3. P. 70-76.

Antipin, V. S.. Andreeva I. A., Kovalenko V. I. Kuznetsov. V. A. Geochemical features of ongonites of the Ary-Bulak massif, Petrology, volume 17, №6, pp. – 601 – 612.,2009

Gramenitskii E. N., Shchekina T. I., Devyatova V. N. Phase relations in fluorine-containing granite and nepheline-syenite systems and the distribution of elements between phases. M: GEOS. 2005. 186 p.

Kovalenko V. I., Kovalenko N. So. Ongonites. M., Science, 1976, 127 p.

Kovalenko V. I.,. Kostitsyn Yu. A.,. Yarmolyuk VV, Budnikov S. V., Kovach V. p., Kotov A. B., Salnikova E. B., Antipin, V. S., magma Sources and the isotopic (Sr and Nd) evolution of rare-metal Li-F granites. Institute of Geology of ore deposits, petrography, Mineralogy and Geochemistry RAS, Petrology, volume 7. M 4. C. 401-429, 1999

Peretyazhko I. S., Zagorsky V. E., Tsareva E. A., Sapozhnikov A. N. Incompressibility fluoride-calcium and aluminosilicate melts in ongonites of the ary-Bulak massif (Eastern Transbaikalia) // Dokl. Russian Academy of Sciences, 2007, vol. 413, no. 2, pp. 244-250

Peretyazhko I. S., Savina E. A.,Fluid-magmatic processes in the formation of rocks in the massif of ongonites of the Ary-Bulak (Eastern Transbaikalia): Geology and Geophysics, vol. 51, no. 10,pp. 1423-1442, 2010.

Peretyazhko I. S., Savina E. A., Dril S. I., Gerasimov N. With. Rb-Sr isotopic system and the features of distribution of Rb and Sr in rocks from the array of ongonites of the Ary-Bulak, basavanna with the participation of the processes the fluoride-silicate magmatic immiscibility, Geology and Geophysics , vol. 52, No. 11, pp. 1776-1789, 2011.

Shchekina T. I., Gramenitskii E. N., Alferyeva Y. O. Leucocratic magmatic melts with extreme concentrations of fluoride: experiment and natural relations // Petrology. 2013. - Vol. 21, № 5. - P. 499-516.

Asavin A.M.[1], Anosova M.I.[1], Gorbunov A.A.[2]., Veksler I.V.[3], Conditions for crystalization and evaluation of the equilibrium of interstitial liquid with cumulus minerals in the eastern Pansky massive layered complex.

[1]Institute of Geochemistry and Analytical Chemistry, Moscow, (aalex06@inbox.ru);
[2]Perm State National University, Perm (art.gor.psu@ya.ru);
[3]Institute of Geology and Geophysics Siberia Academy, Novosibirsk

Abstract. The distribution of rare-earth elements in the basic minerals of the stratified rhythms of the layers platinum reef Fedorovo-Panskoye deposit was studied using LA ICP-MS analysis. We calculated the equilibrium temperatures and fO_2 during evolution of the plagioclase, pyroxene and interstitial melt in the layered platinum-bearing complexes of gabbronorites of the East Pansky Massif on the basis of the rare earth europium geobarometer and a number of other geothermometers. The calculated equilibrium temperatures of the mineral-melt and oxygen fugacity show that within the typical stratified rhythm: (gortonolite)-(olivine gabbro)–(gabbronorites)-(leiko gabbro)-(anorthosite), these parameters changed significantly. This proves that the interstitial melt could be sufficiently fractionated during the formation of magmatic stratification, while trace elements were redistributed between the early minerals of the cumulus and the melt and the accumulation of ore elements took place. A number of numerical models for the accumulation of ore components are given.

Keywords: *layered intrusion, coefficient distributioin trace element, PGE deposit, mafic-ultramafic pluton, magma differentiation*

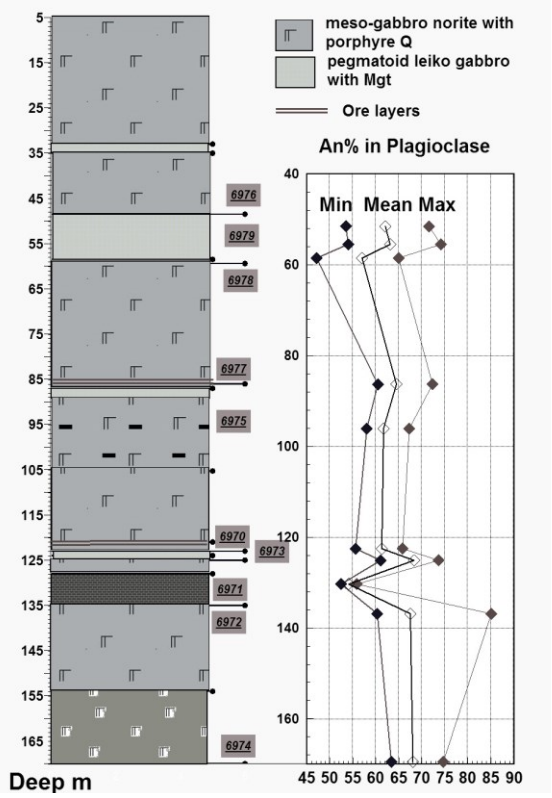

Fig. 1. Section of layered part Pana massive (hole 416). Number sample mark in rectundular frame

Introduction. One of the most important questions of the genesis of stratified massifs is the evolution of the melt composition in the magmatic chamber from the first stage squeeze in the camera melt to the appearance of an interstitial melt in with the cumulus crystal assembles in layered complexes. The concentrations macro components in the parent melt is more or less clear (Davies et al. 1980; Eales et al. 1993; Latypov et al. 2001; Latypov et al. 2007; Wilson 2012], but there is no such clarity about the concentrations of trace elements [Tribuzi et al. 1999; Wilson et al. 1999; Cawthorn 2007; Latypov 2009] yet. The difficulty of solving this problem is that, we have a good knowledge of the way of crystallization of the main melts in the basaltic system, and can estimated the composition parent melt fraction on next stages of evolution by compare composition quenching facies rock, dike complexes, melt inclusions in the main magmatic minerals. But we cannot adequately estimate the change in the composition of the interstitial melt in time with respect to trace elements. Proceeding from the existing models of the genesis of the basic layered complexes, we can calculate the change in the composition of the equilibrium melt to a crystallization level in the chamber of 50-40%. Next stage: there are the simple fractionation model changes to the interaction model of the cumulus zone of early crystals with an interstitial melt, the amount of which gradually decreases to the first percent by the full crystallization of the intrusion camera.

At the same time, mechanisms are realized for the formation of magmatic stratification in different parts of the chamber. We must be used to calculate the fractionation of trace elements more complex model. And it is important, because it is at this stage that ore zones containing sulfides and Pt group elements (PGE) are formed in the layered complexes. However, as in the beginning of the formation of the magma chamber, the content of trace elements in the interstitial melt is determined by the distribution coefficients of trace elements (Kp) between the crystals: Pl, Opx, Ol, Cpx and melt (Liq) and variations this value with depend on changes in temperature and oxygen fugacity during the evolution melts. Therefore, estimating the value of Kp and their variation in the array is a rather important problem. On the example of layered zone "B" of the East Panskiy massif, we estimated the values of Kp plagioclase in the gabbronorites of the layered complex.

Geology and data. The general scheme of sampling is presented in Fig.1. Ore horizons are located closely to the border of rhythms. Rhythm begins with melanocratic gabbronorite and ends with leucocratic gabbro to anorthosite. On the right side on Fig.1 show the graph variation composition of plagioclase in the rock. It can be seen that for each of the parts of the rhythm a fairly wide interval of anorthite content in various grains of plagioclase is characteristic. This proves that even within the same rock there are both early plagioclases of cumulus, and later - equilibrium with the late interstitial melt. Thus, the change in the composition of the plagioclase from the lower part of the rhythm to the upper one is comparable to the variations in the composition within the same layer.

The concentration of trace elements in rocks were obtained by the LA-ICP-MS analysis (analytic from Vernadsky institute GEOKHI Moscow). Concentration full spectrum of rare earth elements in plagioclase were measured. The observed distribution of trace elements in plagioclase is similar to contents An% in plagioclase. On Fig.2 shows linear trend of changes in Ce-La content in plagioclase, it is seen that the lowest levels correspond to the upper parts of the rhythm (leucocratic gabbro and anorthosite) and the highest lower parts - melanocratic gabbronorites. A separate trend is formed by plagioclases from trachi-gabbronorites (one of the earliest cumulus rocks of the lower parts of the rhythm, black asterisks on the Fig.2). They also have elevated barium content. The trend of Sr-Ba is similar to La-Ce, although less pronounced.

To calculate Kp, it is necessary to know the content of a rare element in an equilibrium melt. As a first approximation, we took data on the composition of melt micro inclusions in the plagioclase of the Bushveld Massif [Cawthorn 2007] and the compositions of the model primary melts of Bushveld [Wilson 2012]. There are other works on the evaluation of the compositions of primary magmas, but they do not have such a complete spectrum of contents of rare elements. For the Fedorovo-Pansky massif there are no publications on this topic. Of recent works, mention can be made of the work [Groshev 2011] in which the averaged contents of the rocks of the massif are given, which can be considered as close to the initial composition of the primary magma. Of course, these data are very approximate, but a qualitative picture of the Kp variations can be obtained.

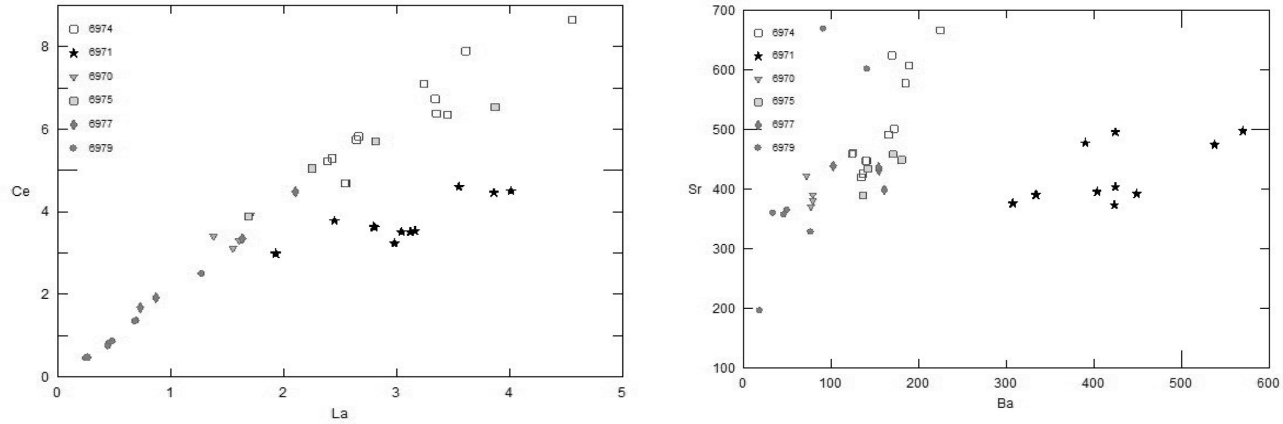

Fig.2. Distribution of trace elements in plagioclases in ppm.

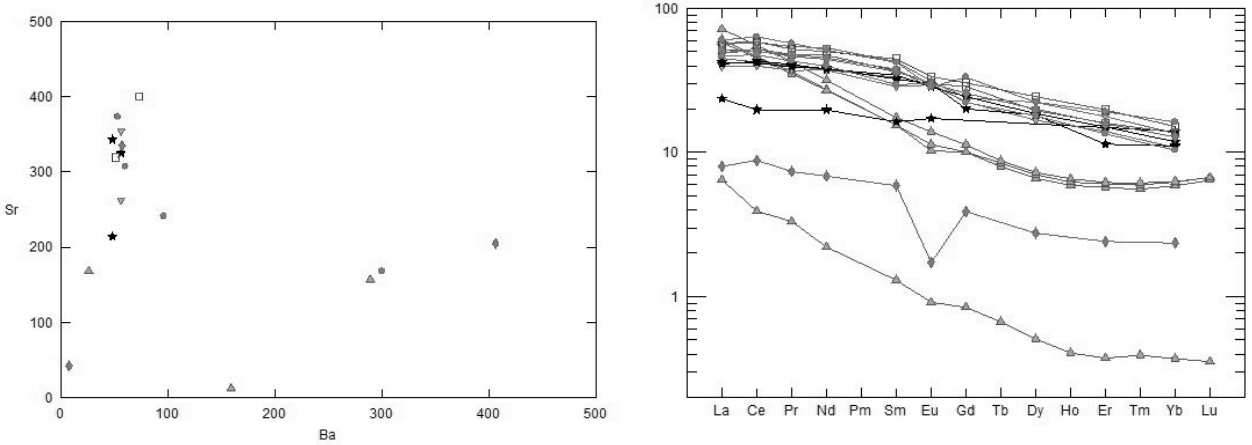

Fig.3. Distribution of rare earth elements in primary melts in ppm [Cawthorn 2007; Wilson 2012;].

Figure 3 presents data on the distribution of trace elements in primary magmas. It can be seen that the parent melts show a very wide range of composition. This is explained the long evolution of melts leads to a significant differentiation and variation of trace elements in the melt.

Calculation of the Kp plagioclase was carried out for Sr, Ba, La, Ce, Eu. The control of the value of Kp was carried out according geothermometers to [Sun et al. 1974, Tepley et al. 2010; Bedard 2006]. Figure 4 shows the temperature calculations by the strontium geothermometer. On Fig.4 shows the variation of Kp. It was possible to calculate the temperature interval by geothermometers from [Sun et al. 1974; Tepley et al. 2010]. The variations of Kp Sr are not significant, since the decrease Kp by temperature factor is compensated by a change in the composition of the plagioclase. The level of concentrations of Ba, La, in model primary melts does not allow calculating reasonable in magnitude. The La content in model melts is about an order of magnitude higher than the content at which real Kp and the corresponding equilibrium temperature can be obtained. The same situation is also observed for Ce, Ba.

The calculated temperatures make it possible to evaluate the fugacity of oxygen (log fO2) in the crystallization of rocks. Figure 5 shows logfO2 calculations for two geooxymeters [Sun et al. 1974; Drake 1075]. It can be seen from the figure (Fig. 5 B) that although there is a systematic difference in calculations, most points are located near the 1:1 line and slightly higher.

This indicates some conclusion can be some done. It is interesting that, in the evolution of each rhythm interval of rocks, value of log (fO2) changes not along the line of some constant oxygen buffer. We observed a significant change in the oxygen regime with a slight temperature change.

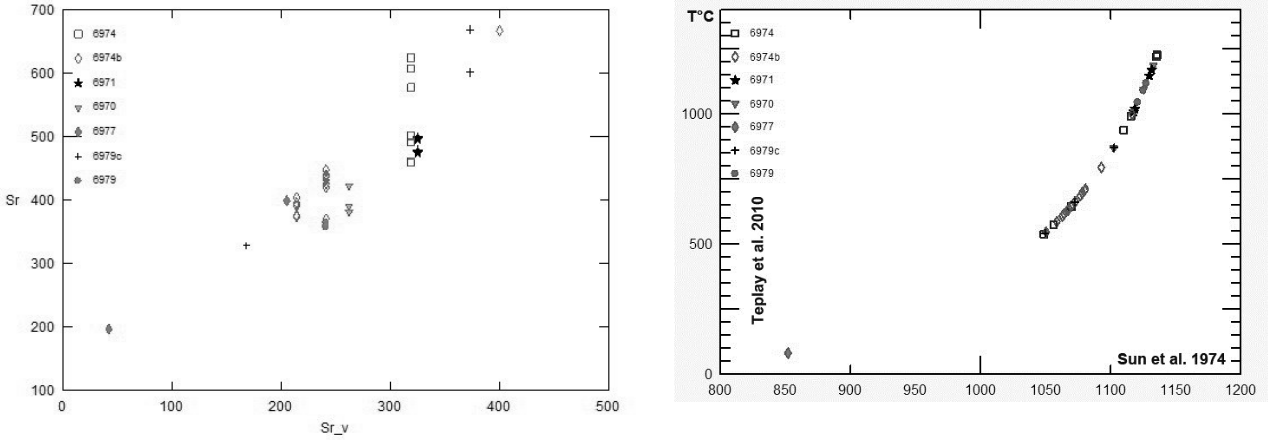

A B

Fig. 4. Distribution of strontium in primary melts in ppm (A). The ratio of the design temperatures T C (B) along the x axis [fSun et al. 1974] and along the y axis [Tepley et al. 2010].

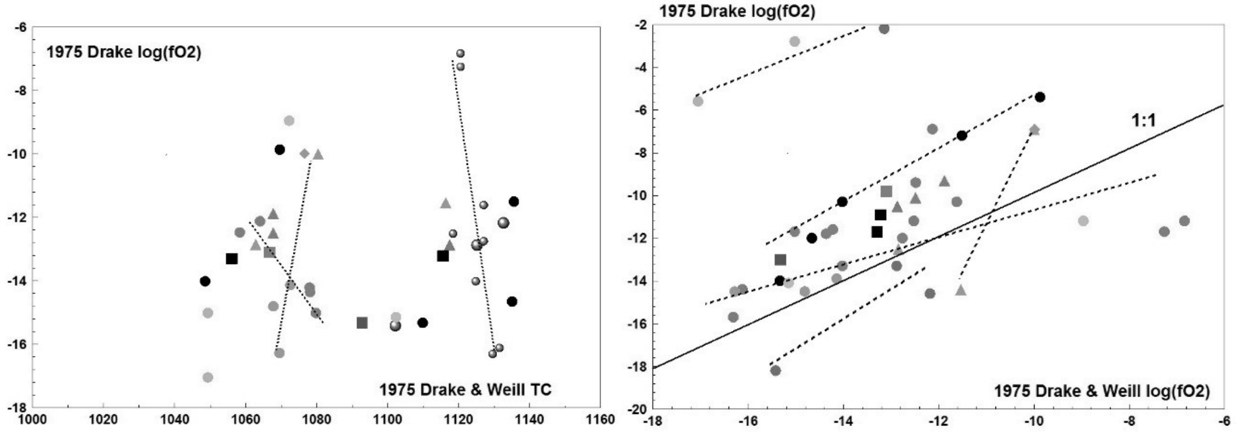

A B

Fig.5. The calculated values of log (fO2) as a function of temperature according to [Sun et al. 1974]. The ratio of calculated log (fO2) obtained from two independent geothermometers [Sun et al. 1974] and [Drake 1975]. Line dotted on the charts show trends within one group of rhythm rocks.

Result. Complexity in the evaluation of parent melt, and the variation of the elemental composition of the interstitial melt exists. With this equivocality, we rely on the calculations of fractionation of trace elements on the one hand, which is reflected in the composition change in plagioclase, and on the other hand on the evaluation of the equilibrium of the plagioclase with the melt.

A qualitative evaluation of the Kp values in the layered complexes of the East Pansky Massif showed that there are certain objective limitations on the composition of the interstitial melt with respect to trace elements. The melt should contain very low levels of the first ten ppm of barium, ten ppm of rare earth elements (La, Ce, Nd) and should be expected by a negative europium anomaly. Concentration in plagioclase relatively low about 300 ppm and less Sr content. All these limits condition to high values of Kp (> 1) and this is the evidence of significant role in the fractionation of plagioclase.

The change in the temperatures of crystallization and the oxidation regime in the melt during the cooling of the intrusion cannot fundamentally change the order of the distribution coefficients and therefore does not change the overall yield. On the other hand, if we assume that the equilibrium of plagioclase and ros-melting is reached, the calculations show the need for significant variations in the fugacity of oxygen within (within) each rhythm element of the stratified series. This is very important, since it proves that the oxidative regime could vary within small distances, and local equilibria could exist long enough. This helped maintain a constant gradient at the boundaries of the rhythms, and therefore the ability to transfer and concentrate the ore components in the melt due to electrochemical forces.

Conclusion An estimate of the oxygen fugacity and the crystallization temperature indicates that in the cumulus at the stage of formation of magmatic stratification fO2 changed very significantly (by 4-6 logarithmic units) even within the individual layers of the rhythm. And this change was not accompanied by a significant change in crystallization temperatures.

References:

Bédard, J.H. Trace element partitioning in plagioclase feldspar //Geochimica et Cosmochimica Acta 2006, 70 (14), P.3717-3742.

Cawthorn, R.G. Models for incompatible trace-element abundances in cumulus minerals and their application to plagioclase and pyroxenes in the Bushveld Complex. //Contributions to Mineralogy and Petrology 1996, V.123(1), P.109-115.

Cawthorn, R. Grant. Cr and Sr: Keys to parental magmas and processes in the Bushveld Complex, South Africa. //Lithos 2007, V.95.3, P.381-398.

Davies, G., Cawthorn, R. G., Barton, J. M., & Morton, M. Parental magma to the Bushveld Complex. //Nature 1980, V.287, P.33-35.

Drake, Michael J. The oxidation state of europium as an indicator of oxygen fugacity.*//Geochimica et Cosmochimica Acta* 1975, V.39, N.1, P.55-64.

Eales, H. V., Botha, W. J., Hattingh, P. J., De Klerk, W. J., Maier, W. D., & Odgers, A. T. R. The mafic rocks of the Bushveld Complex: a review of emplacement and crystallization history, and mineralization, in the light of recent data. //Journal of African Earth Sciences (Middle East) 1993, V.16.1-2, P.121-142.

Latypov, R. M., Mitrofanov, F. P., Skiba, V. I., & Alapieti, T. T. The western Pansky Tundra layered intrusion, Kola Peninsula: Differentiation mechanism and solidification sequence. //Petrology C/C of Petrologiia 2001, V.9.3, P.214-251.

Latypov, R., S. Chistyakova, and Tuomo Alapieti. Revisiting problem of chilled margins associated with marginal reversals in mafic–ultramafic intrusive bodies. //Lithos 2007, V.99.3, P.178-206

Latypov, Rais. Testing the validity of the petrological hypothesis 'no phenocrysts, no post-emplacement differentiation'. //Journal of Petrology 2009, egp031. P.1-23

Sun, C.-O., Williams, R.J. and Sun, S.-S. Distribution coefficients of Eu and Sr for plagioclase-liquid and clinopyroxene-liquid equilibria in oceanic ridge basalt; an experimental study. //Geochimica et Cosmochimica Acta 1974, V.38 (9), P.1415-1433.

Tepley, F. J., Lundstrom, C. C., McDonough, W. F., & Thompson, A. Trace element partitioning between high-An plagioclase and basaltic to basaltic andesite melt at 1 atmosphere pressure. //Lithos 2010, V.118.1, P.82-94.

Tribuzio, R., Tiepolo, M., Vannucci, R., & Bottazzi, P. Trace element distribution within olivine-bearing gabbros from the Northern Apennine ophiolites (Italy): evidence for post-cumulus crystallization in MORB-type gabbroic rocks. //Contributions to Mineralogy and Petrology 1999, V.134.2-3, P.123-133.

Wilson, Allan H. A chill sequence to the Bushveld Complex: insight into the first stage of emplacement and implications for the parental magmas. //Journal of Petrology 2012, V.53, N.6, egs011. P.1123-1168

Wilson A. H, Lee C. A. Brown R. T. Geochemistry of the Merensky reef, Rustenburg Section, Bushveld Complex: controls on the silicate framework and distribution of trace elements //Mineralium Deposita 1999, V.34 P.657-672

Asavin A.M.[1], Chesalova E.I.[2] Numerical model for genesis of magmatic complexes of the guli pluton as evidence of differentiation process of a unique primary melt. UDC 552.325;553.212

[1]Institute of Geochemistry and Analytical Chemistry, Moscow, (aalex06@inbox.ru)
[2] Vernadsky Geological State Museum RAS Moscow (chesalova_ei@mail.ru)

Abstract. The genesis of the largest ultrabasic polyphases Guli pluton, located on the northern edge of the Anabar shield of the alkaline ultrabasic Maimecha-Kotui province, is considered. Inspite of the large number of works on the problem of the formation of this alkaline-ultrabasic pluton and similar polyphase intrusions from other alkaline provinces, the question of the composition of the primary melt and the genetic relationship of the pluton-constituent intrusive derivatives remains unresolved. One of the possible answers find the way of forming a mineralization in intrusive is the building model of melts differentiation in magmatic chambers and the processes of fractionation and concentration of rare and ore elements To calculate the models of crystallization differentiation, we applied the method of finding the mass balance by the method of least squares. We used this approach to construct the model of the formation of the Guli ultrabasic alkaline intrusion and of the Konder massif. The control of calculations was also carried out on the basis of an estimate of the exposed areas of different magmatic complexes, quantitatively estimated by to the GIS project of the structure of the Guli and Konder plutons. These numerical models were discussed as evidence of the existence of a common for all intrusive phases of parental magma.

Keywords. *Alkaline ultrabasic pluton, melelitic rock, meimechite, picrate, differenciation model.*

Introduction. Our work examines the genesis of the largest ultrabasic polyphase Guli pluton (Fig. 1), located on the northern edge of the Anabar Shield of the well-known ultrabasic alkaline Maimechi-Kotuy province [Egorov 1969]. Despite the large numbers of articles about Guli rocks and about the genesis similar polyphase alkaline ultrabasic intrusions, the lot of questions remain unresolved. Main of them are the composition of the primary melt and the genetic association of the pluton-constituent intrusive derivatives. One of the possible ways of finding an answer to these questions is the construction of the models for differentiating melts in magmatic chambers and numerically calculating the processes of fractionation. Such models make it possible to identify the most promising ore stages of the ore formation. Trace elements distribution can explain the evolution of the magmatic system.

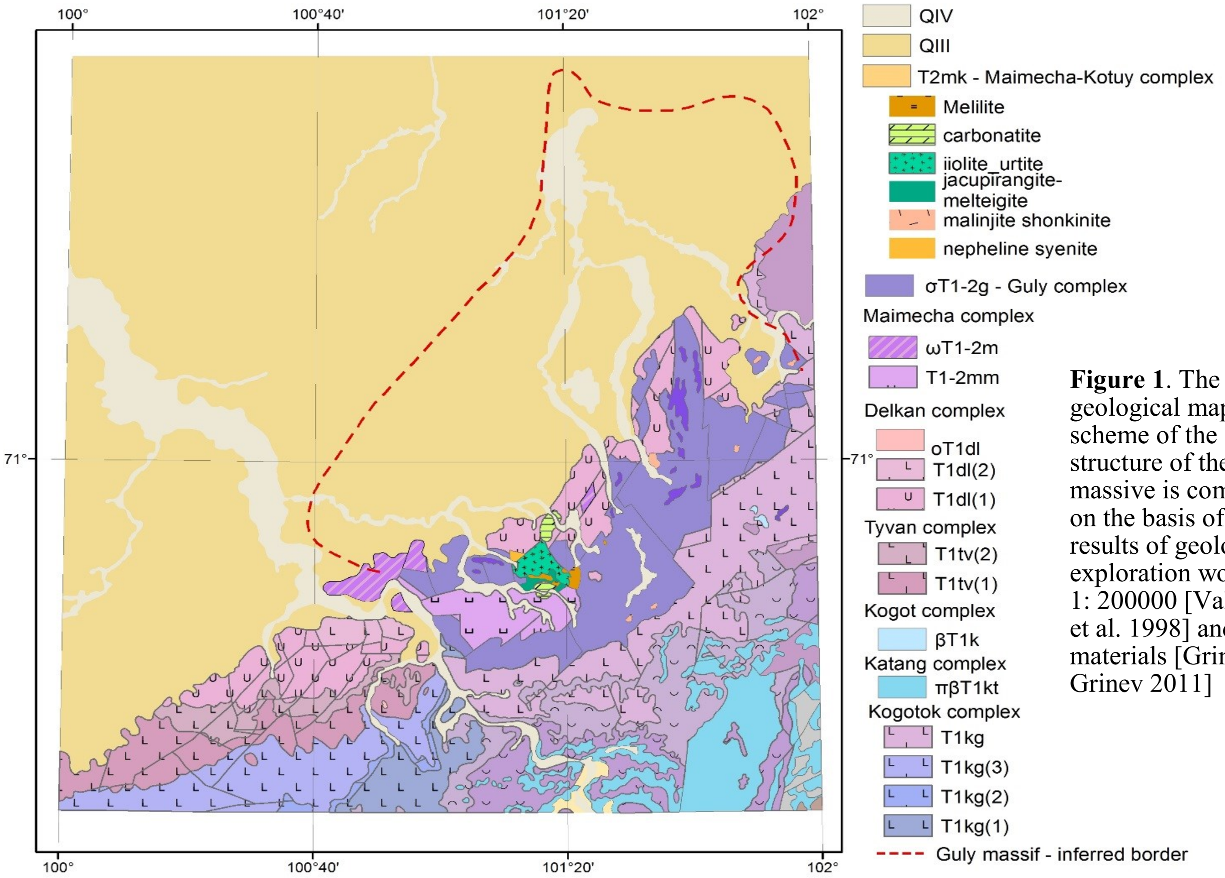

Figure 1. The geological map-scheme of the structure of the Guli massive is compiled on the basis of the results of geological exploration works M 1: 200000 [Valetov et al. 1998] and materials [Grinev & Grinev 2011]

To calculate the models of crystallization differentiation, we used mathematical methods for finding the mass balance in the system. The algorithm of calculation use the method of least squares. In studies on volcanic differentiation series, this method was used in the calculation of fractionation due to separation of minerals of phenocrysts and rest melt and gave excellent results for understanding of their genesis. We attempted to apply this approach to construct a model for the formation of ultrabasic alkaline intrusion.

Method and primary data. The result of the model is the mass balance over all major petrogenic components between the observed intrusive phases and the initial parent melt. This calculation simulates the evolution of a closed system, the composition of which initially fits into the composition of the primary melt. Technically the model is a mathematical solution to a system of redefined equations. The number of equations corresponds to the number of components, and the number of variables corresponds to the number of independent phases participating in the model. The mathematical solution is using the algorithm of finding the least residual by the method of least squares. The root-mean-square residual should be less than the error in determining of the phase fraction in the equation.

One of the basic postulates of the computational model is the closure of the system. There is an initial composition corresponding to the initial state of the system, which then in the processes of fractionation and evolution breaks up into a series of intrusive phases of different composition. Such initial melts compositions are so-called primary magmas. The composition of primary magmas is usually corresponds to not differentiated high-magnesia melts, which can be in equilibrium with the mantle substance, the partial melting of which allows to obtain a huge volume of the primary melt. These magmas fill the interstitial pores space combine with the crystallizing minerals and fractionated and the different portions of the crystal-melt had separate as a mixture of complex liquid, eventually solidifying into as a sequence of intrusive phases.

As the basis of the model, we used the averaged compositions of the intrusive phases of the Guli pluton [Egorov 1991] and the Kondersky massif [Nekrasov et al. 1994]. The compositions are shown in Table 1. This methodic, to estimate the average compositions of intrusive phases in models, is explained by very large variations of the contents of macro components even within one type of rock. These variations can be caused by the secondary alteration processes on the already solidification rocks, or the processes of intra-phase magmatic differentiation, which can, under local conditions, lead to own trends of fractionation of each of the intrusive phases. This phenomenon is very typical for the intrusive phases of the Guli pluton [Egorov 1969]. For example, in the melilitic phase, a complete trend of differentiation is: (Ol + Mell) → - (Ol + Mell + Cpx) → - (Mell + Cpx + Neph) → (Mell + Neph + Sn). The same reason also determines the low accuracy of calculations, which allows us to obtain qualitative rather than quantitative results. Obviously, when constructing a general generalized model of massif formation, such "independent" fractionation trends are difficult to take into account, they obstruct the calculation of a general balance and for them it is necessary to carry out additional calculations at the next stage, when will be calculate a more detailed models.

Table 1. Compositions of rocks used in the calculation of the model Guli pluton (wt% of oxides).

Rock-derivate	n	SiO_2	TiO_2	Al_2O_3	Fe_2O_3	FeO	MnO	MgO	CaO	Na_2O	K_2O	Ref.
Dunite	19	35.93	0.43	0.58	6.14	7.77	0.18	38.71	0.84	0.13	0.06	1
Ore Pyroxenite – kosvite	6	38.33	4.58	3.61	8.88	11.48	0.17	13.68	18.05	0.42	0.03	1
Turjaite	6	36.62	4.72	8.54	0	15.04		7.97	21.52	3.52	1.96	2
Kugdite	3	37.83	1.84	3.78	6.84	7.65	0.09	26.64	14.63	1.01	0.3	3
Jacupirangite	6	36.48	6.31	5.85	10.14	6.91	0.23	9.36	19.19	1.53	1.23	1
Melteigite	4	43.01	2.32	10.99	5.91	5.33	0.27	7.96	14.03	4.51	3.14	1
Malignite	2	45.26	2.96	16.24	5.93	4.79	0.15	3.2	7.45	6.56	3.68	1
Shonkinite	3	43.63	5.42	11.04	9.91	6.27	0.28	4.21	11.16	2.75	3.17	1
Melano ijolite	3	43	2.53	15.64	4.79	3.2	0.16	6.26	11.02	6.49	3.56	1
Ijolite		45.17	3.19	19.93	4.38	2.59	0.19	2.86	7.42	8.77	3.99	1
Nepheline-syenite		53.57	1.15	20.64	4.2	1.5	0	0.75	2.5	7.35	6.21	1
Alkaline syenite	3	59.69	1.16	12.47	3.91	1.93	0.13	2.18	5.21	3.5	8.53	1
Alkaline syenite-aplite		64.84	0	18.28	0.74	0.29	0	0.23	0.22	1.72	14.08	1
Phoscorite	4	12.01	1.37	1.03	18.05	9.38	0.67	9.94	28.32	0.2	0.22	1

Reference: 1- Egorov 1991, 2 - Egorov 1969, 3 - Russ 2000

Table 2. Rock compositions used in calculating the model Konder pluton (wt% oxides) [Nekrasov et al. 1994]

Rock-derivate	n	SiO_2	TiO_2	Al_2O_3	Fe_2O_3	FeO	MnO	MgO	CaO	Na_2O	K_2O
Dunite with Chromite socket	76	38.58	0.08	0.46	4.03	6.13	0.27	45.8	0.39	0.05	0.01
Olivine pyroxenite - pyroxenite (free-ore)	18	49.67	0.45	1.61	2.67	6.48	0.21	19.06	18.9	0.29	0.06
Olivine pyroxenite – Ore-pyroxenite	12	41.04	1.5	2.7	12.69	8.4	0.24	14.15	18.02	0.29	0.12
Melano- gabbro	4	42.61	1.73	9.1	7.64	9.4	0.32	9.23	14.5	2.03	1.25
Olivine pyroxenite	3	48.81	0.59	2.42	1.51	8.02	0.23	18.79	18.41	0.34	0.06
Amphibole gabbro	4	48.61	0.59	17.43	2.44	3.45	0.14	11.53	8.44	4.22	0.31
Phlogopite -Ap-Mgt pyroxenite	20	36.07	2.12	4.84	12.09	8.05	0.31	12.52	18.18	0.7	1.27
Monzonite-diorite	8	61.81	0.72	15.14	2.31	4.36	0.12	2.73	5.07	3.76	2.73
Syenite	17	61.57	0.41	17.35	2.91	0.81	0.07	1.49	2.19	8.44	2.99
Nepheline-syenite	17	55.03	0.94	17.85	4.92	1.75	0.14	1.53	3.66	7.02	4.57

It should be noted that in first we tried (as in the models of volcanic series) to use in calculations only the compositions of minerals from the rocks. But we were not able to obtain any reality results. Then we tried to use in the calculations the directly composition of the rocks as a whole. The petrological meaning of using the composition of intrusive phases as a whole instead of minerals is that the intrusive rock can be a product of the cumulative process occurring under the influence of gravitational and hydrodynamic separation of phases crystallizing in the melt (i.e., the accumulation crystals which sedimentation or flotation in the crystal differentiation processes). Geological and petrographic features of intrusive rocks often do not allow unequivocally establishing to what type of process the given rock belongs. Therefore, using only minerals in modeling, we cannot take into account these very significant part of magmatic chambers components (interstitial melts), which leads to large errors in model. In addition, post-cumulus phenomena, the evolution of interstitial melts, play an important role in the intrusive camera process. They can subsequently separate and give their own independent branch of differentiates during evolution. All this leads to the fact that for an intrusive process, unlike a volcanic process, it is not possible to build an adequate model, based only on the compositions of the crystallizing minerals.

In addition to Gili, we also calculated the model for the formation of the Kondersky intrusion (Table 2, Fig.2). Compositions of rocks are taken from work

[Nekrasov et al. 1994]. In contrast to the Gulinsky pluton, in Konder intrusion chromite bodies appear at an early stage, bodies of alkaline gabbroids are present, and melilithic phases are absent. Comparison of models allows us to get a more complete picture of the realities of our calculations.

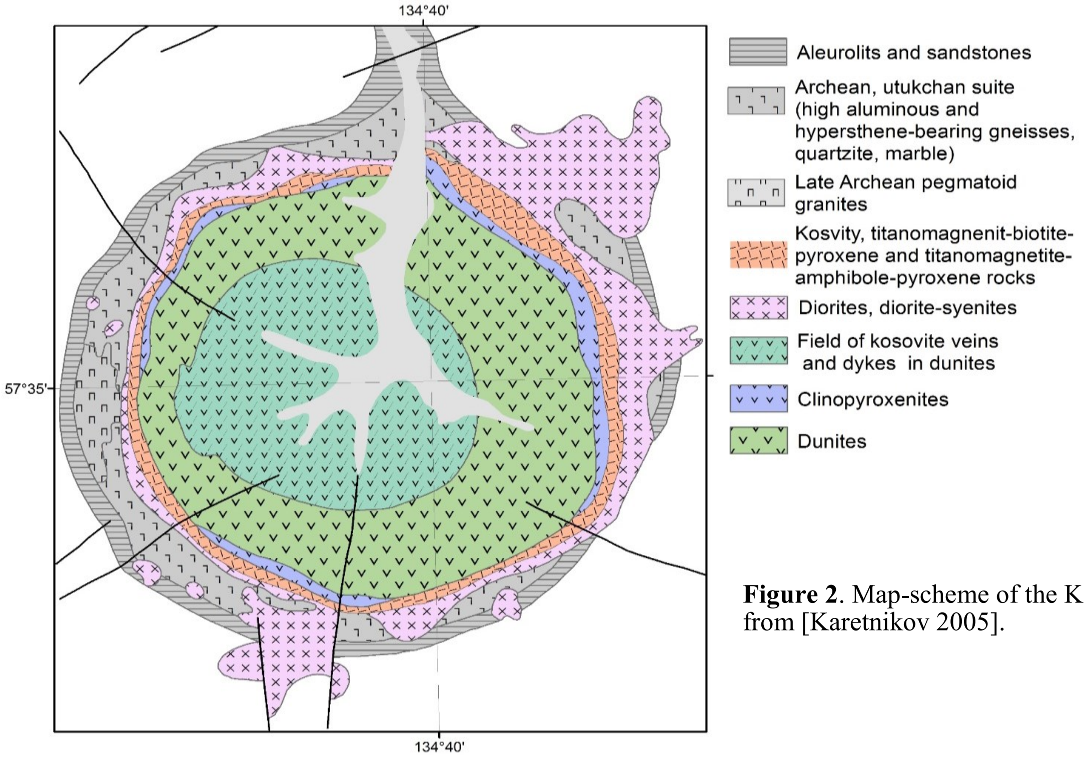

Figure 2. Map-scheme of the Konder massif from [Karetnikov 2005].

The main difference of our work from other studies of the inner structure of ultrabasic intrusions is the development of GIS projects based on available geological maps. Having prepared the GIS projects, we were able to accurately estimate the size of the area of intrusive derivatives into intrusions, their volume relationship. In this way we can compare the volumes obtained in the numerical calculations with the actually observed geological structure. This gives us an additional tool for assessing the realism of the constructed our models of differentiation.

Composition of the parent melt. With such approach in construction of intrusion genesis model, the choice of the composition of the parent magma is critical important. This composition of the parent magma determines, in which part of the multicomponent phase diagram the start point for differentiation put on and begins the process of differentiation, what cotectic associations of minerals will crystallize and in which direction, and to which eutectic points the residual melts will moved. Since there is currently no generally accepted opinion on the composition of the magma that formed the Guli pluton, we used several variants of the compositions of such magmas. We make choice from the actually observed in the nature subvolcanic and volcanic rocks or glasses from melt inclusions in firstly magmatic minerals (olivine, pyroxene).

These are additional geological evidences of realistic our numerical model and the existence of a connection between hypothetical primary melts and intrusive rocks of the Guli complex. We used the following types of vulcanite, extended in the region of the Guli pluton: meimechite dykes, alkaline picrite dykes (Maymechinskaya sequence), mela-nephelenites (Arydzhan volcanic series), melilitic nephelenites (Arydzhan volcanic series). In addition, we used the composition of the primary melt, evaluated in the work by the results of homogenization of melt inclusions from olivine of the Guli turjaite [Russ and Plechov 2000].

Parent melts on the base of picrite and meimechite composition. It is not easy task to choose melt composition with the using of high magnesium lavas.

One of the traditional solutions of this problem is the use of the mean arithmetic value of the meimechite or picrite lavas from set analysis of samples. However, it seems to us that the presence of a wide range of the compositions of these ultrabasic volcanites is a reflection of the real geological process of the formation of these melts, and therefore it is impossible not to take this phenomenon into account in the model. The reasons for the dispersion of primary melts compositions may be the different degrees of partial melting of the mantle or fractionation-accumulation of olivine crystals when the magma rises to the surface. Figure 3 shows the variations in the compositions of meimechite and picrite melts in the coordinates of MgO-(Na_2O + K_2O)-CaO-Al_2O_3. The figures show not only the total composition of rocks, but also the compositions of the groundmass of these volcanites. It can be seen from the figure that there is a fairly wide range of compositions, and the trends of these volcanites partially overlap. Therefore, the choice of the primary melt composition that corresponds to meimechite, and even more to picrite melt, is not so simple and requires discussion.

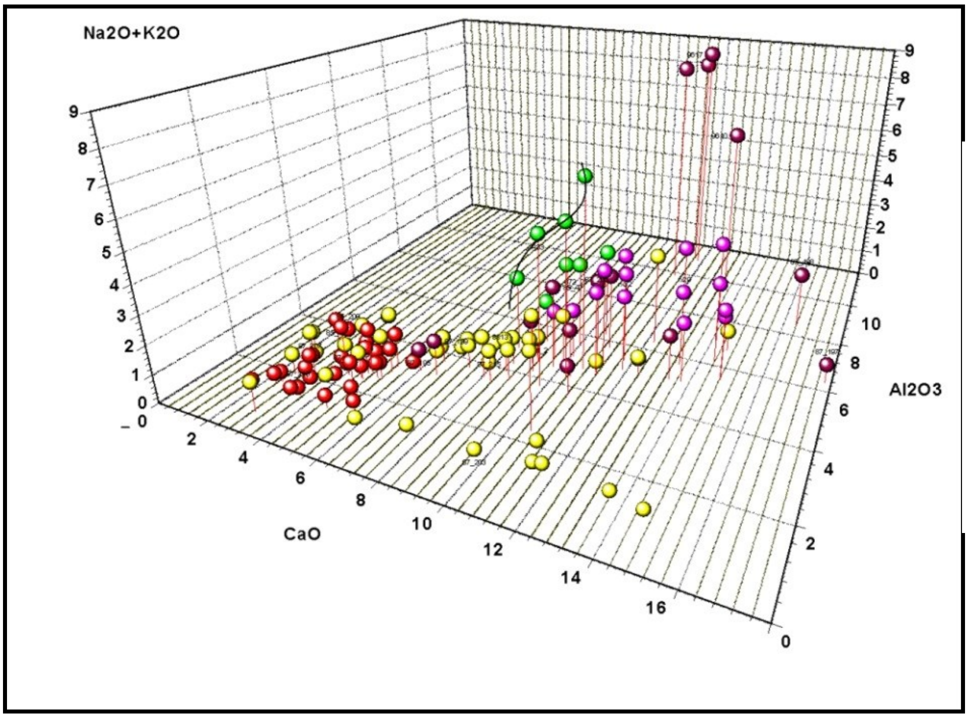

Figure 3. Compositions of rocks and groundmass of picrites (brown and pink) and meimechites (red and yellow). The green dots show the experimental glass compositions obtained from the melting of meimechite [Elkins-Tanton et al., 2007].

Although the ratio of Ca/Al in rocks is close, but the absolute level of calcium concentration is much higher in picrites. In general, the picrites are strongly enriched in Ti and Ca, therefore, on the 3D-diagram of CaO-Al_2O_3- (Na_2O + K_2O), the picrite evolution trend points are shifted relative to the meimechite trend into the calcium region. Of great interest are the results of the Linda Elkins-Tanton experiment with co-authors [Elkins-Tanton et al., 2007]. In the Fig 3, these compositions are marked with green dots. It is evident that although these authors describe this composition as a meimechite one, it is actually a picrite one. And the trend of evolution of this composition at high pressure reflects a significant increase in alkali content in the melt.

We used in the calculations several extreme (start and end point on trend line) compositions from the existing samples of meimechites and picrites. In Tab.3 shows all the variants of the compositions of the used meimechite melts. The use of extreme compositions (by the fractionation trend) in calculations allows one to estimate the stability of the model with with greater reliability select one or another type of primary melt.

Table 3. Compositions of primary magmas used in the model (wt% oxide).

Rock-derivate	code in model	SiO_2	TiO_2	Al_2O_3	Fe_2O_3	FeO	MgO	CaO	Na_2O	K_2O	Ref.
meimechite	Mod1	41.64	2.58	2.86	4.74	7.93	33.25	5.31	0.19	0.65	2
	Mod2	39.38	3.36	3.44	3.79	9.5	24.78	8.38	0.31	0.78	
	Mod3	40.88	2.34	2.8	4.28	8.23	35.19	4.82	0.21	0.47	
picrite	Pcr1	41.34	4.64	5.06	4.65	7.9	17.04	13.37	0.13	1.44	
	Pcr2	39.76	5.22	6.28	5.03	8.54	11.76	17.82	0.52	0.15	
	Pcr3	39.7	3.26	5.23	5.72	9.79	22.85	8.83	1.21	1.52	
Given composition for the Konder massif. close to meimechite	Prim_K	42.49	0.42	2.95	4.81	6.23	33.39	5.03	0.74	0.56	1
Composition glass in inclusions from olivine of turjaite of the Guli	Tur1	35.06	5.43	11.23	8.17	0.25	4.66	21.00	8.48	3.14	3
	Tur2	38.46	2.78	8.94	12.44	0.18	5.69	20.62	6.02	2.46	

The reference: 1- Nekrasov et al. 1994; 2 - Egorov 1991; 3- Russ and Plechev 2000

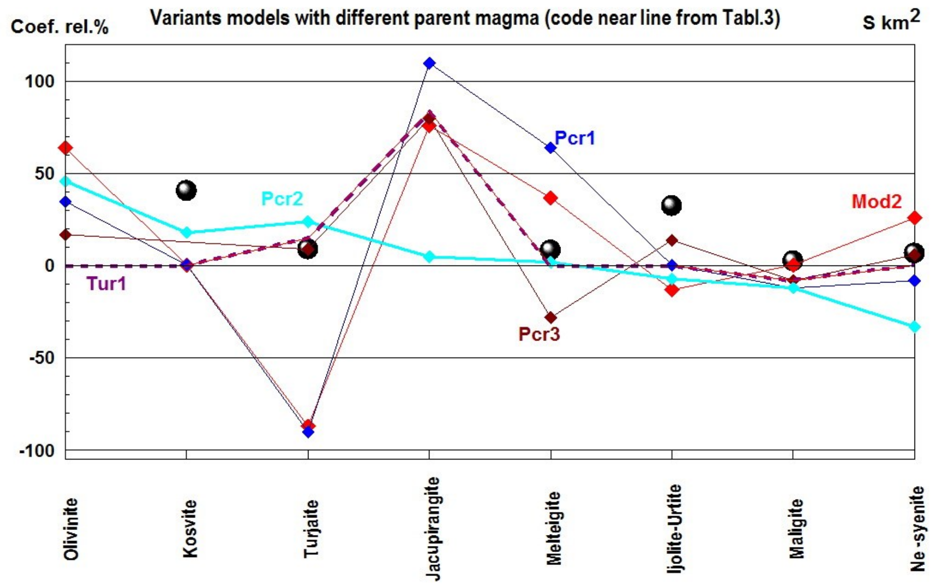

Figure 4. Comparison calculation coefficients in model (color markers for five models code as in Tabl.3) with the observed areas (S km^2) of rocks derivates in the Guli massive.

Result of calculation In this paper, we do not give complete table results of calculations, because the volume of the paper is limited. Only the best final result is shown in the graph (Fig. 4). First of all, attention is drawn to the fact that in models for the Guli pluton, it is necessary to use negative coefficients to obtain an agreed mass balance of some intrusive phases.

This is the very mention difference between the calculations for the Konder massif and Guli. In the model for Konder, we found surprisingly good solution. The discrepancy error is very small, and all intrusive phases have positive coefficients. And even the volume derivates relationship in the model corresponds to the geological relationship observed in the geological map.

The overwhelming volume is occupied by the dunite phase (more than half by weight), the remaining phases approximately having the same volumes. Phoscorite and syenites are of secondary role. But if we exclusion alkaline derivates (syenite, monzonite) from model - then model don't have solution. This emphasizes that the alkaline nature of the evolution of the primary melt on the Konder magmatic camera. Differentiation cannot do without the formation of the intrusive phases of increased alkalinity.

A completely different result is observed in the calculations for the Guli model. The evolution of meimechite melts does not allow obtaining alkaline intrusive phases of the Guli pluton. The calculated coefficient in model for these derivates is negative. In addition, if we remove the alkaline phases from the calculation, the fraction of peridotite becomes extremely low, which does not correspond to the area spread kosvite and olivine pyroxenite observed on the geological map.

It is also interesting to emphasize that attempts to calculate only the rocks of the first subphase also did not help to find solutions. We used a three-phase equation with ore pyroxenites, melteigite and dunite. However, the residual error remained extremely high. Thus, it can be assumed that modern meimechite melts could not be the parent magma for the Guli pluton as a whole and even for its ultrabasic part.

Table 4. Model fractions of intrusive phases and observed area intrusive subphases on the Guli pluton.

Derivate	Code parent magma (from Tabl.3)						Area*	
Subphase fraction (rel. %)	Mod2	Pcr1	Pcr2	Pcr3	Tur1	Tur2	km^2	%
Olivinite	64	35	46		17		359	
Kosvite			18				15.5	40.7
Turjaite	-87	-90	24	42	9	15	3.5	9
Jacupirangite	76	110	5	37	78	84		
Melteigite	37	64	2	70	-28		3.2	8.4
Ijolite Urtite	-13		-7	-18	14		12.3	32.5
Malignite		-12	-12	21	-6	-8	2.6	2.6
Nepheline-syenite	26	-8	-33	-56	6		1	6.8
Carbonatite							5.9	

* the relative % of area are calculated without taking into account olivinite and carbonatites.

One of the ways to solve this paradox may be the participation of additional subphase, such as chromite cumulus deposit. If this assumption is correct, then would such "extra" phase would have a important role in the formation of ore deposits on the massive. Such type of rock we can observe on Bor-Uryakh massive Maimecha-Kotui province.

When we use picrite melts in the model, it was possible obtain the better results than in the case of meimechite magmas. However, in that variant, it was not possible to calculate the fully satisfactory derivate phase intrusive sequence. Although there are variants with an acceptable magnitude of the error discrepancy, negative coefficients appear in them for nepheline-containing phases. And although field of these rocks is not very great on the Guli massif (ijolites, alkaline syenite), however our data do not allow us to speak about the convergence equations for model for alkaline intrusive phases.

In the best case, a discrepancy error value 1.23 is obtained, and the coefficient for nepheline syenite is -15. It should also be noted that the calculated volume of dunite in this case is much lower than observed (about 50%), and there are very large values of the coefficients of alkaline (turjaite, malignite) intrusive phases. It is important to note that the result of calculations is possible to obtain rocks of the melilitic intrusive phase. That is the evidence that larnite normative magmas have their own special primary melt and cannot be obtained from other types of parent magma. On the contrary, we performed calculations with high-calcium melts detected in micro inclusions (Tabl. 3). [Russ & Plechev 2000]. It is obvious that these melts are not initial for other of intrusive phases of the Guli pluton. In addition to the turjaite itself, their evolution cannot produce any other intrusive phase.

Overall, calculations show that picrite melts do not allow the formation of an enormous large dunite core of the Guli pluton.

Chemical composition of picrite melt (unsaturated in silicon and with high calcium) product derivate two volume of ultrabasic on one volume of melilite phases during the evolution of this magma. Similar relationships are observed, for example, in the Kugda massif. It is too early to talk about the place of the ore process in the evolution of picrite melts. High discrepancies in the system calculation indicate the possibility of the appearance of additional petrochemical types of melts. For example, it can be carbonatites, phoscorite melts. These low silicate magmas can help to found the mass balance in the model genesis of the massif.

Conclusion. Our calculations of the petrochemical model made it possible to obtain qualitative results of the formation of the massif. For the first time we have estimated the possibility of obtaining the all-main derivate intrusive phases, observed on the Guli and Konder, during the evolution of a single primary melt. The entire spectrum of such primary melts from ultramafic meimechites to melilite nephelinite was used in our calculations.

The result showed, that the types of initial magmas of the Gulinsky pluton, proposed today, could not fully explain its evolution. The model, obtained from meimechite melts, better explain the geological structure of the massif, however, picrite magmas make it possible to explain the formation of more alkaline intrusive phases. Model of high calcium melts for turjaite magmas explain a local melilite-bearing branch of the evolution of the system, from them it is impossible to obtain other types of alkaline rocks noted on the massif. Thus, a more attractive hypothesis is the existence of several primary magmas.

The constructed electronic maps made it possible to compare the areas of exit of the intrusive phases to the surface escape and to estimate their fractions in the computational models. The share of the ultrabasic nucleus in plutons is several times higher than expected in calculations. The ratio of the remaining phases to each other is perfectural agreement with model. The exception is more acidic differentiates - ijolite-urtites, malignites, nepheline syenites. GIS models of the structure of arrays allowed to link numerical theoretical models to specific geological structures of the structure of intrusive bodies.

In general, convergence of calculations does not allow speaking about a satisfactory model based on available data.

References:

Valetov A.V., Yu.G. Kosmayenko, Yu. K. Krakovetsky Group geological survey of scale 1: 200000 in the northern part of the Siberian platform on the Gulinskaya area within the sheets R-47-XI, XII. 1998, 340p. // Report of the Polar Party of the PGP "Norilsk Geology" for 1990 -1996. Talnach (cyrilic)

Grinev O.M., P.O. Grinev New data on morphotectonics, material composition and ore content of the Gulin volcano-pluton // Platinum of Russia. Collection of scientific works. Krasnoyarsk. 2011. 564 with. Red DA Dodin. 2011,. T VII, .C.356-378

Zhabin A.G. On the structure and sequence of formation of the Gulinsky dunite complex of ultrabasic and ultrabasic alkaline lavas of alkaline rocks and carbonatites / / in the book. Petrology and geochemical peculiarities of the ultrabasite complex of silk rocks and carbonatites M. Nauka 1965, p.159-192

Egorov L.S. Iiolite-carbonatite plutonism // M .: Nedra, 1991, 258 p.

Egorov L.S. Melilit rocks of the Maimecha-Kotui province // L .: Nedra, 1969, 249 p.

Nekrasov I.Ya., Lennikov A.M., Oktyabrsky R.A., Zalishchak B.L., Sapin V.I. Petrology and platinum content of calcium alkaline-ultrabasic complexes. Moscow: Nauka, 1994. 378 p.

Russ I.T., Plechov P.Yu. Inclusions of melts in olivine olivine-melilite rocks, the Guli massif, north-west of the Siberian platform. // Reports of the Russian Academy of Sciences, 2000, vol.375, N3, p. 384-389.

Kogarko L.N., Ryabchikov I.D. (1995) Conditions for the generation of meimechite magmas (Polar Siberia) by geochemical data // Geochemistry. 1995. № 12. P. 1699-1709.

Nekrasov I.Ya., Lennikov AM, Oktyabrsky RA, Zalishchak BL, Sapin V.I. Petrology and platinum content of calcium alkaline-ultrabasic complexes. Moscow: Nauka, 1994. 378 p.

Elkins-Tanton L.T., D. Draper, C. Agee, J. Jewell, A. Thorpe, P. Hess, The last lavas erupted during the main phase of the Siberian flood basalts: Results from experimental petrology,// Contributions to Mineralogy and Petrology, 2007, Vol. 153 No 2, pp. 191-209.

Azarova N.S.[1], Bovkun A.V.[1], Nosova A.A.[2], Garanin V.K.[1] Clinopyroxenes and chrompshinelides from the heavy fraction of kimberlite rocks of Kimozero (Karelia)

[1]M.V. Lomonosov Moscow State University, Department of Geology, Moscow,

[2] Institute of Geology of Ore Deposits, Petrography, Mineralogy and Geochemistry, Russian Academy of Sciences, Moscow (nadiya-azarova@mail.ru)

Abstract. Presents results of a study of the morphology, phase and chemical composition of clinopyroxene and chrome spinel from the early Proterozoic kimberlite pipe, Kenozero (Karelia). The clinopyroxenes are represented by diopside (Mg# 84.6-93.7; Ca# 44, 6-49, 7) containing 0.5 to 3.5 wt.% Cr_2O_3. About 12% of chrome spinel belong to the diamondiferous dunite-harzburgite paragenesis. Dominated by clinopyroxene and chromespinelides are lherzolite paragenesis. Among the disseminated chromespinel grains with high content of titanium.

Keywords: *Kimozero pipe, kimberlite, oxide minerals, spinel, diopside, Karelia*

The early Proterozoic kimberlites of the Kimozero, located within the Karelian craton, are among the most ancient indigenous manifestations of diamondiferous rocks. The age of their formation corresponds to 1986±4 million years (Samsonov et al., 2009). The main indicator minerals of kimberlites of these - chromespinelides are and ilmenite, in very small amounts are present in pyrope and clinopyroxene (Ustinov et al., 2009). The composition of the latter is characterized weakly.

Studied the morphology and chemical composition of clinopyroxene and chrome spinel from heavy fraction of kimberlites of Kimozero.

Among the studied clinopyroxene grains of size < 0,5 mm dominated (about 70%) colored in emerald green, much less common pale and dark green. Most of the grains are transparent. More than half of the sample consists of fragments and split grains, the rest – whole and damaged grains. The majority of the grains has an irregular form, 17% is grain with elements of cut, 16% - round-oval. The surface of most grains is rough, much less common smooth and with pyramidal-tiled relief. One third of the grains have fragments of a fine-grained "shirt" dark or light color (Fig.1).

Among of chrome spinel (<0.5 mm) are the most common fragments of octahedra with vicinale and corroded surface.

42 grains of clinopyroxenes and 46 grains of chrome spinel by a method of X-ray microanalysis the chemical composition.

Almost all the studied clinopyroxenes are represented by diopside (Mg# Of 84,6-93,7 Per; Ca# 44,6-49,7) (Fig. 3A) with a mixture of jadeitic and cosmochronology minerals, varying in content of Cr_2O_3 (0,5-3,5 wt.%), Al_2O_3 (0,3-2,2 wt.%), TiO_2 (0-0,4 wt.%) and Na_2O (1-2,6 wt.%) (Fig. 2). According to the classification (Arkhangelsk..., 1999) the composition of clinopyroxene corresponds to diopside mantle weakly diamondiferous uniformly granular lherzolites, websterites and pyroxenites (± ilmenite).

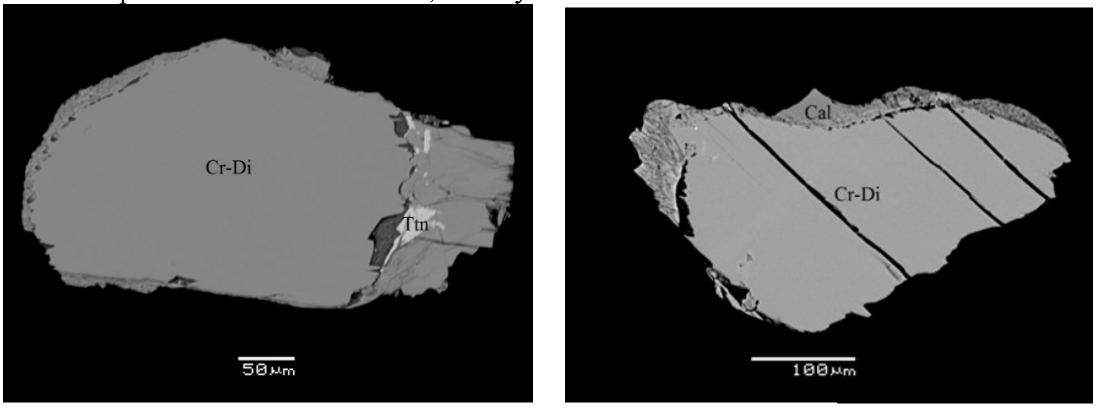

a b

Fig. 1. Clinopyroxene grains with fine-grained titanite-chlorite (a) and carbonate (b) "jacket". Images in reflected electrons.

Found that diopside with high Na_2O contents (2,3 to 2,6 wt.%) related to the paragenesis and uniformly granular lherzolites and garnet-clinopyroxene-chromespinellids splices, is characterized by a constant admixture of TiO_2 (about 0,3-0,4 wt.%) and Cr_2O_3 (1,8-3,5 wt.%). One of the grains (1.5 wt. % Cr_2O_3; 1.6 wt. % Al_2O_3; 1.1 wt. % Na_2O) is similar in composition to the diopside inclusions in diamond (Arkhangelsk..., 1999). In General, about 88% of the studied sample consists of grains containing > 1 wt. % Cr_2O_3. Dominates (45%) diopside with Cr_2O_3 content from 1.5 to 2.5 wt. %. Number of grains containing > 3 wt. % Cr_2O_3, is about 14%. Individual grains are characterized by high contents of FeO_Σ (~11мас. %) at a very small amount of Cr_2O_3 (0,1 wt. %) and Na_2O (up to 0,1 wt. %). For them, Mg# and Ca# represented 73,2 at 73,7 metric and 35,1 at 35,9, respectively.

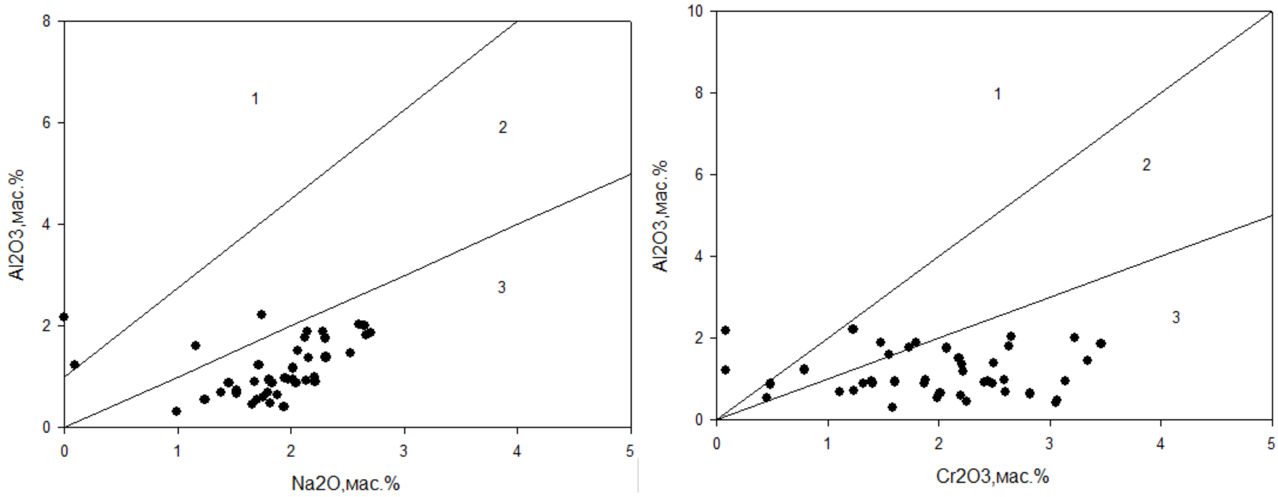

a b

Fig. 2. Composition diagrams for clinopyroxene from kimberlites of Kimozero. The numbers indicated by region: 1 – spinel-pyrope facies and spinel-pyrope subfacies; 2 – grospiditical subfacies; 3 – coesite subfacies (Sablukov et al, 2000)

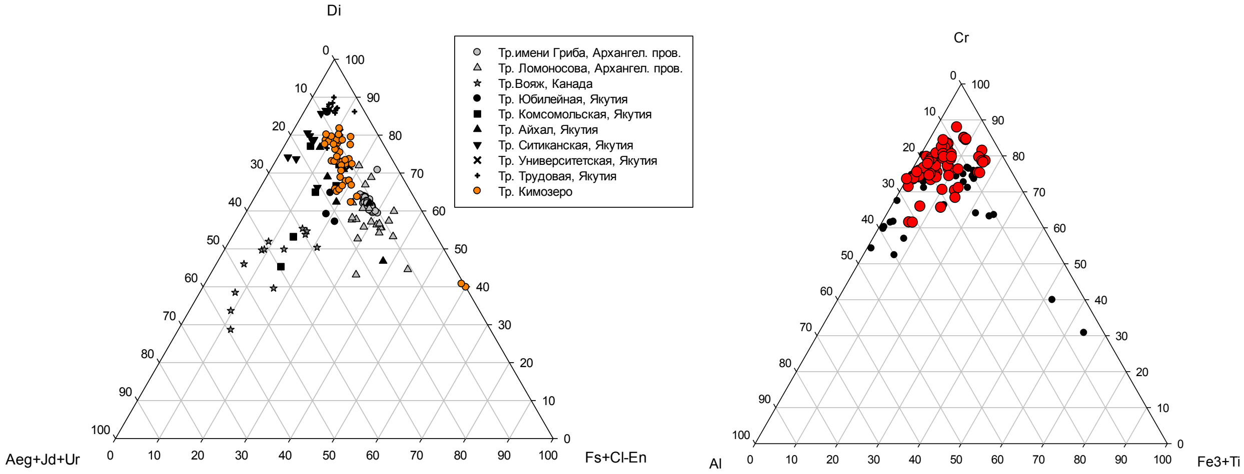

a b

Fig. 3. Chart compositions for clinopyroxene (a) and chromespinellids (b) from kimberlites, Kenozero. For fig. a data for clinopyroxene from kimberlites of the World (Kargin et al., 2017; Kudryavtseva et al., 2005; Smart, 2017; Ashchepkov et al., 2016, 2017) in Fig. b used black circles indicated points of composition of chrome spinel from kimberlites, according Kenozero (Putintseva and Spiridonov, 2017)

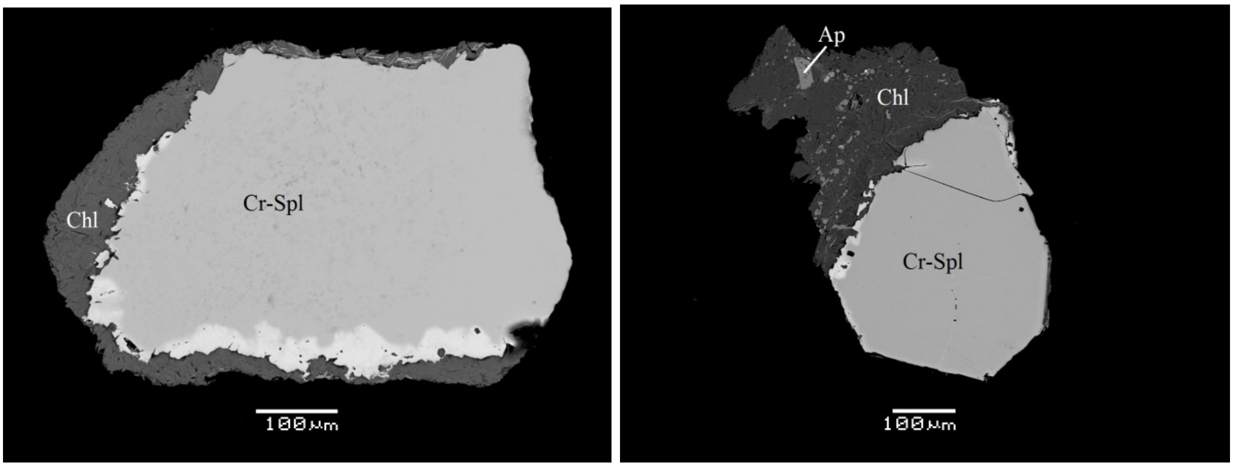

a b

Fig. 4. Grains of chrome spinel are enriched with FeO, MnO and ZnO boundary zones and chlorite by adhesions. Images in reflected electrons

The charts in the coordinates Na_2O-Al_2O_3 and Cr_2O_3-Al_2O_3 (Fig. 2) figurative points of compositions of the studied clinopyroxenes are mainly situated in the field of high pressure subfacies depths (34-40 kbar).

Comparison of the chemical composition of the studied clinopyroxenes from the tube, Kenozero with the composition of this mineral from kimberlites of Zolotistogo, Vertinskogo and Kopinskogo fields of the Arkhangelsk diamondiferous province revealed their similarity (Fig. 3A). In kimberlites named fields, more than half (55-69%) samples make up the clinopyroxenes from equigranular lherzolites (Arkhangelsk..., 1999). In addition, clinopyroxenes of these objects generally have a reduced aluminum content compared to clinopyroxene from kimberlites of other diamond-bearing provinces.

About 12% of the studied grains of chrome spinel composition (Cr# 81-93, up to 0.6 wt. % TiO_2, 10-13 wt. % MgO) corresponds to chromite of diamond-bearing dunites and harzburgites. The predominant (75%) ranging in composition (Cr# 66-93, up to 2.6 wt.% TiO_2, 9.7-13.5 wt.% MgO) chromespinelides are lherzolite paragenesis. Some grains (about 8%) are enriched with TiO_2 (3, 7-4, 8 wt. %) and Fe_2O_3 at Cr# 81-94. Peripheral areas of most of the grains amount of MgO is sharply reduced, increasing the content of FeO, there is a mixture of MnO and ZnO (Fig. 4).

Thus, the results of these studies suggest that the clinopyroxenes and the chromspinells from kimberlite rock Kenozero manifestations are predominantly in the lherzolite paragenesis. Among the disseminated chrome spinel grains with high content of titanium. Chromite of diamondiferous dunite-harzburgite paragenesis is about 12%.

References:

Atlas. Morphogenesis of diamond and minerals-satellites in kimberlites and related rocks of the Arkhangelsk kimberlite province. - 1st ed. – M.: Polar. Cu., 2005,624.

Arkhangelsk diamondiferous province (Geology, petrography, Geochemistry and Mineralogy) / edited By O. A. Bogatikov, Moscow state University, 1999, 524 p.

Putintseva E. V., Spiridonov, E. M., the Oldest in Russia diamondiferous kimberlites and metacommunity of Chemothera, Karelia // proceedings of the Universities. Geology and exploration. 2017.

Sablukov S. M., sablukova L. I., M. V. Shavyrina Mantle xenoliths from the kimberlite deposits of rounded diamonds Simpering district, the Arkhangelsk diamond-bearing province // Petrology. 2000. Vol. 8. No. 5. P. 518-548.

Samsonov A.V., Larionova Yu., Salnikova E. B., and others, Isotope Geochemistry and geochronology of Paleoproterozoic kimberlites Kenozerskoye manifestations (Karelia). In the book.:Mate. Ivross. Conf. isotope. geochronol. SPb. 2009. P. 158-161.

Ustinov V. N., Zagainyi A. K., Smith, K. B., etc. Early Proterozoic diamond-bearing kimberlites of Karelia and the peculiarities of their formation // Geology and Geophysics. 2009 Vol. 50. No. 9. P. 963-977.

Ashchepkov I.V., Kuligin S.S., Vladykin N.V. et. Comparison of mantle lithosphere beneath early Triassic kimberlite fields in Siberian craton reconstructed from deep-seated xenocrysts // Geosience Frontiers 7 (2016), p. 639-662

Ashchepkov I.V., Logvinova A.M., Ntaflos T., et. Alakit and Daldyn kimberlite fields, Siberia, Russia: Two types of mantle sub-terranes beneath central Yakutia? // Geosience Frontiers 8 (2017), p.671-692

Kargin A.V., Sazonova L.V., Nosova A.A. et. Sheared peridotite xenolith from the V. Grib kimberlite pipe, Arkhangelsk Diamond Province, Russia: Texture, composition, and origin // Geosience Frontiers 8 (2017), p.653-669

Smart K.A., Tappe S., Simonetti S.S. et. Tectonic significance and redox state of Paleoproterozoic eclogite and pyroxenite components in the Slave cratonic mantle lithosphere, Voyageur kimberlite, Arctic Canada // Chemical Geology 455 (2017), p. 98-119

Koptev-Dvornikov E.V., Bychkov D.A.. Equations for the calculation of the contents of small components (Mn, Ca, Cr) in olivine in equilibrium with melt.

M.V. Lomonosov Moscow State University, Department of Geology, Moscow (ekoptev@geol.msu.ru)

Abstract. In order to develop a system of equations designed to calculate the equilibrium of olivine with a melt, the results of 669 "dry" quenching experiments were processed using multidimensional statistics. Each experiment is characterized by temperature, pressure, oxygen fugacity, phase compositions. The range of compositions of melts varies from komatiite basalts to dacites. The data is extracted from the INFOREX database.

The obtained equations reproduce the contents of small components in experimental olivine with an error (in mass %) not exceeding for MnO ± 0.01, CaO ± 0.04, Cr_2O_3 ± 0.03 at a significance level of 95%.

Keywords: *olivine, silicate melt, equilibrium, equation, thermobarometer, modeling.*

In order to develop a system of equations designed to calculate the equilibrium of olivine with a melt, the results of 669 "dry" quenching experiments were processed using multidimensional statistics. Each experiment is characterized by temperature, pressure, oxygen fugacity, phase compositions. The range of compositions of melts varies from komatiite basalts to dacites. The data is extracted from the INFOREX database.

The task was to derive such equations that would be suitable for use in a wide range of compositions of basic systems. After considering a number of approaches to the calculation of the composition of the system in the calculation of the equilibrium constant, EV Koptev-Dvornikov and DA Kuznetsov. Bychkov (Koptev-Dvornikov, Bychkov, 2007) dwelled on the following form of the equation of the liquidus thermobarometer:

$$\ln K = \frac{A+\beta P}{T} + B + CT + D\lg fO_2 + E\ln\left(\frac{\mathrm{Al}}{\mathrm{Si}}\right) + FW + \sum_{i=1}^{n} J_i X_i \quad (1),$$

where K is the reaction constant for the formation of a minal of any crystalline phase; P is the pressure in kbar; T is the absolute temperature; fO_2 is the volatility of oxygen in bars, $W=\ln((\mathrm{Na+K})\mathrm{Al}/\mathrm{Si}^2)$, X_i is the molar fraction of the i-th component of the melt, and n is the number of components considered.

The parameters Al/Si and W (they are calculated using atomic amounts of elements) are proposed (Ariskin, Barmina, 2000) for the refinement of olivine and plagioclase thermobarometers, respectively. A, β, C, D, E, F, J_i are coefficients for the corresponding variables, B is a constant. The basis for finding these coefficients is the principle of using methods of multidimensional statistics. The thermodynamic meaning of these constants follows from the form of the known physicochemical equations: $A \sim \Delta H/R$, $\beta \sim -\Delta V/R$, $\{B + CT + D\lg fO_2 + E\ln\left(\frac{\mathrm{Al}}{\mathrm{Si}}\right) + FW + \sum_{i=1}^{n} J_i X_i\} \sim -\Delta S/R$, where ΔH, ΔV and ΔS are the enthalpy, volume and entropy effects of the phase reaction, R is the universal gas constant.

Both in natural samples and in olivines from our sample, the standard microprobe analysis continuously reveals, besides the main oxides, the presence of MnO, CaO and Cr_2O_3 in amounts reaching the first percent. In this regard, the compositions of olivines are recalculated into 5 minals - forsterite $MgSi_{0.5}O_2$ (Fo), fayalite $FeSi_{0.5}O_2$ (Fa), tephroite $MnSi_{0.5}O_2$ (Tep), larnitie $CaSi_{0.5}O_2$ (Lrn) and chromolivine $CrSi_{0.5}O_2$ (CrOl) - postulates all Cr in the melt in a divalent form.

The formation of the above minals from the melt occurs as a result of the following heterophase reactions:

$$MgO^l + 0.5SiO_2^l = MgSi_{0.5}O_2^{Fo},$$
$$FeO^l + 0.5SiO_2^l = FeSi_{0.5}O_2^{Fa},$$
$$MnO^l + 0.5SiO_2^l = MnSi_{0.5}O_2^{Tep},$$
$$CaO^l + 0.5SiO_2^l = CaSi_{0.5}O_2^{Lrn},$$
$$CrO^l + 0.5SiO_2^l = CrSi_{0.5}O_2^{CrOl}.$$

Equation (1) implies the form of equations for calculating the mineral content of minerals. Example for forsterite minal:

$$X^{Fo} = \exp\left[\left(A^{Fo} + \beta^{Fo}P\right)/T + B^{Fo} + D^{Fo}\lg fO_2 + E^{Fo}\ln\left(\frac{\mathrm{Al}}{\mathrm{Si}}\right) + \sum J_i^{Fo} X_i + \ln\alpha_{MgO} + 0.5\ln\alpha_{SiO_2}\right] \quad (2),$$

where a_i is the activity of the initial components in the melt according to the two-lattice melt model by Nielsen with co-authors (see Frenkel et al., 1988).

The corresponding form has expressions for the remaining minals. Finding the coefficients for the variables (optimization) was done by minimizing the squares of the differences between the calculated and experimental minal contents using the "solver" add-on in the MS Excel program (Table 1).

On the graphs of Fig. 2 shows the correspondence between the experimental and calculated contents of the minerals.

One of the statistically valid criteria for the quality of thermobarometers is the size of the confidence interval at a given level of reliability of the linear regression between the experimental and calculated values. The advantage of confidence intervals for estimating the quality of an equation, in comparison with, for example, standard deviations, is their clarity and the fact that the confidence interval narrows with increasing sample size.

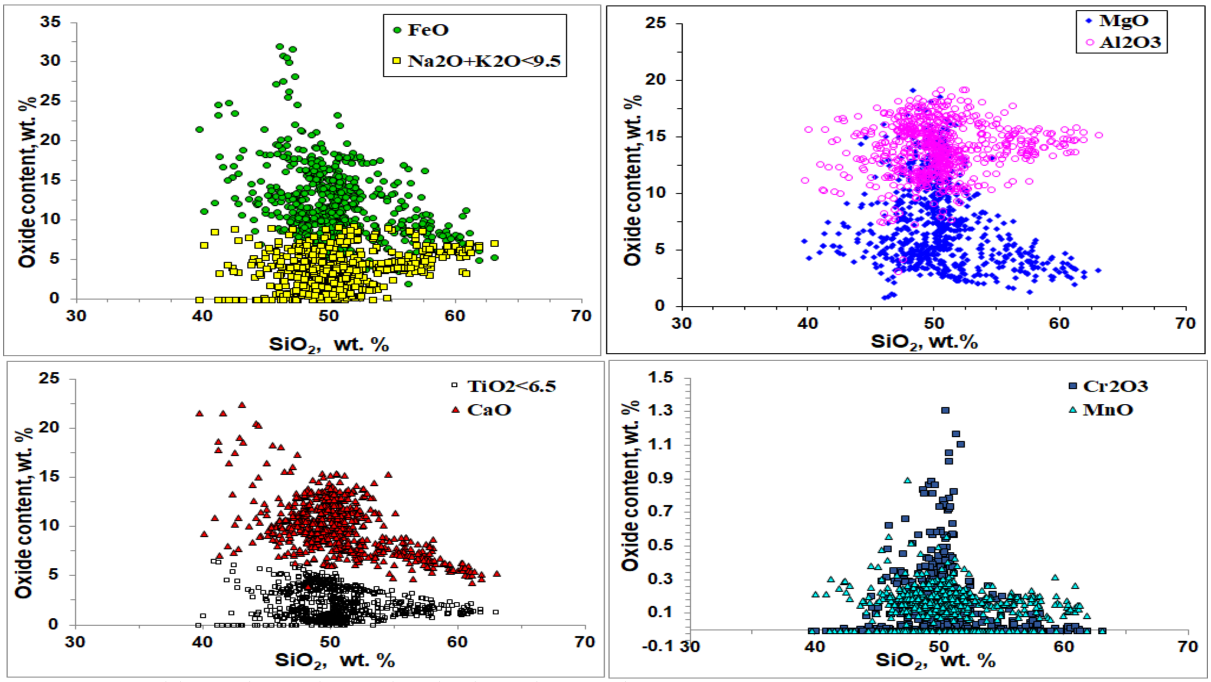

Fig.1. Compositions of experimental melts from the sample.

Table 1. Values of the coefficients and constants for equations of the form (2), found using the add-in "solver" in the MS Excel program for olivine minals.

	Fo	Fa	Tep	Lrn	CrOl
A	2025,429	5962,05	4457,813	5887,654	0
β	0,846666	16,3266	7,284742	14,35791	-39,9058
B	-2,302	-3,8401	-2,98328	-17,7041	0,157348
D	0,010035	0,007344	0,023556	0,025759	-0,01323
E	0,238653	0,042771	0,192141	0,4634	-0,2567
J_{Si}	2,696381	0	0	9,950438	-3,44026
J_{Ti}	4,434315	0	0	7,544974	-4,33736
J_{Al}	2,481555	0	0	4,703435	4,543982
J_{Fe}^{3+}	3,131638	0	-6,97429	7,125565	4,821374
J_{Fe}^{2+}	2,827177	0	2,439437	15,41908	0,396911
J_{Mn}	0	0	0	0	
J_{Mg}	0	0	-2,15514	10,977	0,48629
J_{Ca}	3,832335	0	2,114766	17,09586	-0,75603
J_{Na}	1,83251	0	0,085677	15,53179	0,678457
J_{K}	5,228879	0	3,350357	21,26928	2,015494
J_{Cr}	0				-40,798

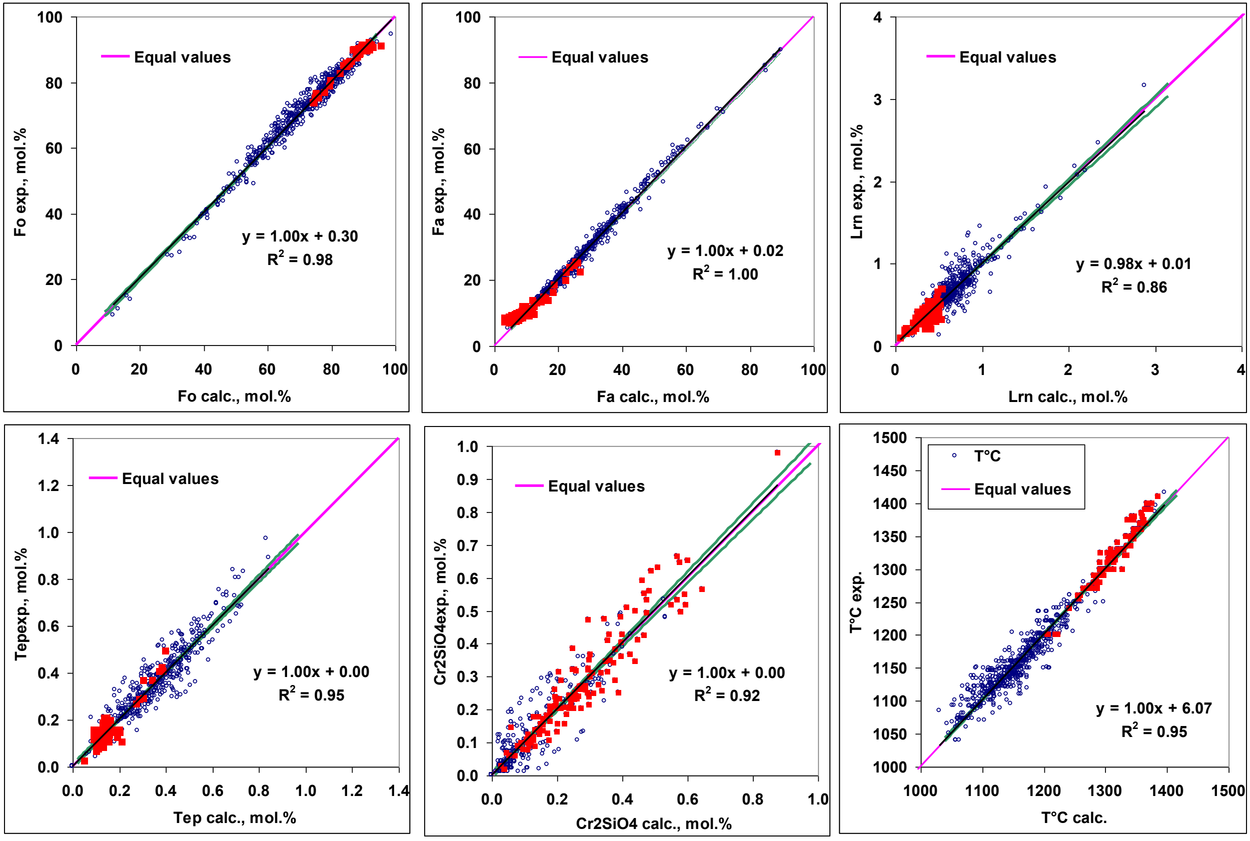

Fig. 2. Correspondence between the calculated and experimental contents of olivine minals and liquidus temperatures. Green curves - boundaries of confidence intervals at 95% reliability level. Red marked high-pressure experiments.

For clarity of comparison of calculated and experimental contents of small elements, calculated concentrations of minerals were recalculated to weight percent of oxides. Fig. 4-6 shows the contents of Mn, Ca and Cr in olivine, calculated by two methods: a) through equations of the form (2) with the parameters from Table 1 and b) through the distribution coefficient K_D, which was determined for the sample in question by dividing the contents of Mn, Ca and Cr in olivine by the content of these elements in coexisting melts.

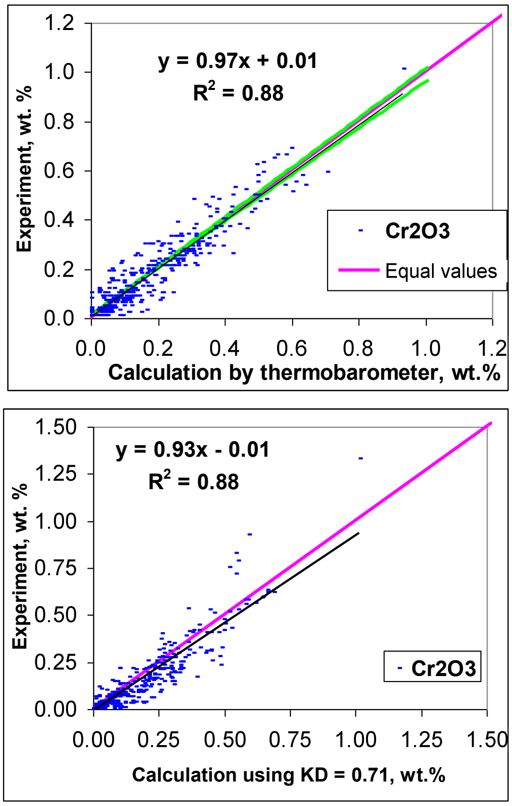

Fig. 3. Comparison of the experimental and calculated in two ways the contents of Cr_2O_3 in olivine.

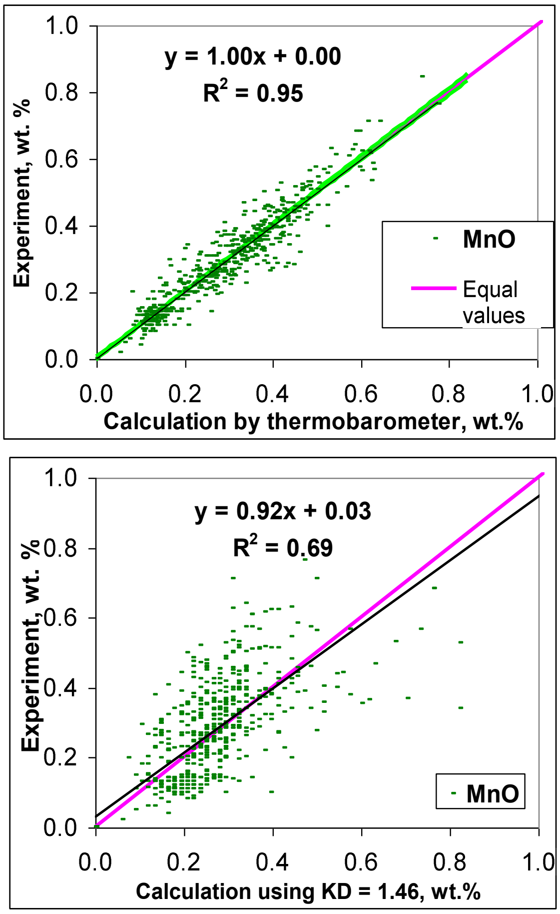

Fig. 4. Comparison of the experimental and calculated in two ways the content of MnO in olivine.

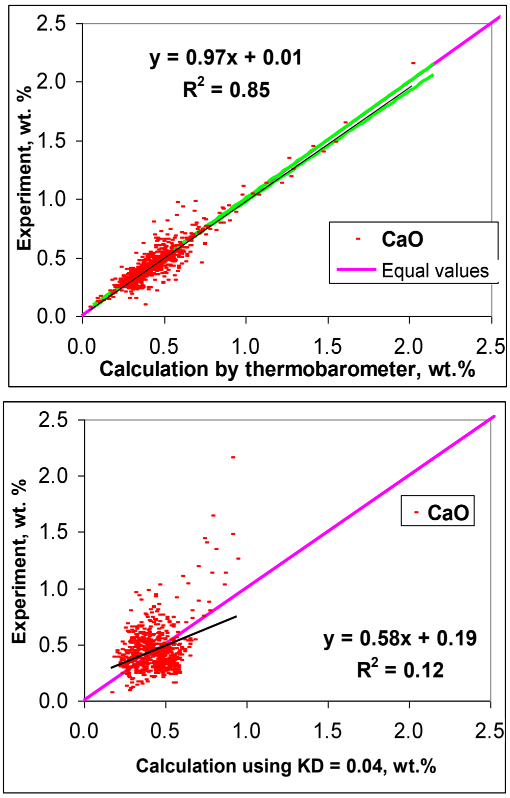

Fig. 5. Comparison of the experimental and calculated by two methods of CaO content in olivine.

In the series of Cr_2O_3, MnO, CaO, the results of the predictions with the help of K_D concentrations of these oxides sharply worsen, while calculations with equations of the form (2) remasin at a high level. The error in predicting the contents of Cr_2O_3 does not exceed ± 0.03 mass. % at 95 percent reliability level, MnO ± 0.01 mass. %, CaO - ± 0.04 wt. %, MnO – ± 0.01 масс. %, CaO – ± 0.04 масс. %. This circumstance will allow us to model the fractionation of these elements with a higher accuracy, which may prove useful, for example, in geochemical thermometry procedures.

Acknowledgements. The authors are grateful to AA Ariskin, GS Barmina and GS Nikolaev for their selfless efforts to create and update the INFOREX database.

References:

Ariskin A. A. et al. INFOREX information retrieval system: analysis and processing of experimental data on phase equilibria in igneous rocks //Petrology. – 1997. – vol. 5. – №. 1. – p. 28-36.
Koptev-Dvornikov EV, Bychkov DA Geothermometers for a wide range of compositions of basites: Mat. Conf. "Ultramafite-Mafite Complexes of Pre-Cambrian Folded Regions." Irkutsk. Izd. SB RAS, 2007. P. 178-181.
Frenkel M.Ya., Yaroshevsky AA, Ariskin AA, Barmina GS, Koptev-Dvornikov EV, Kireev BS Dynamics of intra-chamber differentiation of basite magmas. Moscow: Nauka, 1988. 216 c.

Koptev-Dvornikov E.V., Bychkov D.A.. Equations for the calculation of the contents of small components (Fe, Mg, K) in plagioclase in equilibrium with melt.

M.V. Lomonosov Moscow State University, Department of Geology, Moscow (ekoptev@geol.msu.ru)

Abstract. In order to develop a system of equations for calculating the equilibrium of plagioclase with a melt, the results of 445 "dry" quenching experiments were processed using multidimensional statistics. Each experiment is characterized by temperature, pressure, fugacity of oxygen, phase compositions. The range of compositions of melts varies from basalts to dacites. The data is extracted from the INFOREX database.

The calculation of the stoichiometric composition of the plagioclase converges when Si, Al, Ti, and Fe are involved in the carcass-forming motif, hence iron is predominantly in the trivalent form.

The obtained equations reproduce the contents of small components in experimental plagioclases with an error (in weight%) not exceeding for FeO ± 0.08, for MgO ± 0.04, for K_2O ± 0.03 at a significance level of 95%.

Keywords: plagioclase, silicate melt, equilibrium, equation, thermobarometer, modeling.

In order to develop a system of equations for calculating the equilibrium of plagioclase with a melt, the results of 445 “dry” quenching experiments (407 single-atmospheric and 38 high-baryon) were processed using multidimensional statistics. Each experiment is characterized by temperature, pressure, volatility of oxygen, phase compositions. The range of compositions of melts from basalts to dacites (Fig. 1). The data was extracted from the INFOREX database (Ariskin et al., 1997).

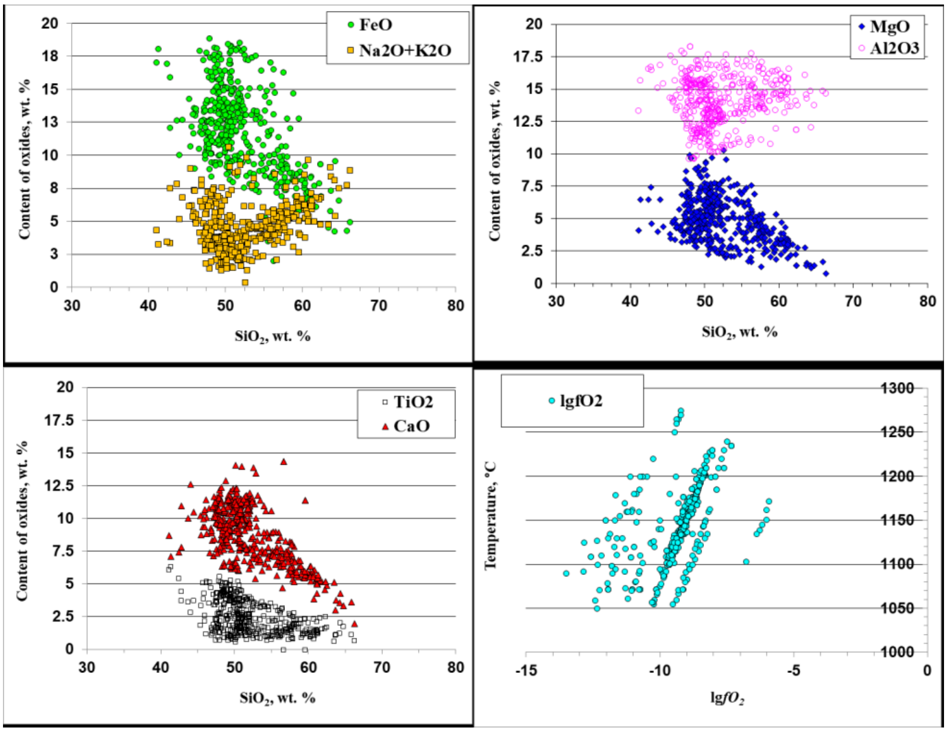

Fig.1. Compositions of experimental melts and lgfO_2 from the sample.

The problem was the derivation of such equations that could predict the composition of plagioclase, including the contents of small components, over a wide range of compositions of basite systems. After considering a number of approaches to the calculation of the composition of the system in the calculation of the equilibrium constant, EV Koptev-Dvornikov and DA Bychkov (Koptev-Dvornikov, Bychkov, 2007) dwelled on the following form of the equation of a liquidus thermobarometer:

$$\ln K = \frac{A+\beta P}{T} + B + D\lg fO_2 + E\ln\left(\frac{\mathrm{Al}}{\mathrm{Si}}\right) + FW + \sum_{i=1}^{n} J_i X_i \qquad (1)$$

where K is the reaction constant for the formation of a minal of any crystalline phase; P is the pressure in kbar; T is the absolute temperature; fO_2 is the volatility of oxygen in bars, W=ln((Na+K)Al/Si_2), X_i is the molar fraction of the i-th component of the melt, and n is the number of components considered. The parameters Al/Si and W (they are calculated using atomic amounts of elements) are proposed (Ariskin, Barmina, 2000) for the refinement of olivine and plagioclase thermobarometers, respectively. A, β, D, E, F, J_i are coefficients for the corresponding variables, B is a constant. The basis for finding these coefficients is the principle of using methods of multidimensional statistics. The thermodynamic meaning of these constants follows from the form of the known physicochemical equations: $A \sim \Delta H/R$, $\beta \sim -\Delta V/R$, $\{B + D\lg fO_2 + E\ln\left(\frac{\mathrm{Al}}{\mathrm{Si}}\right) + FW + \sum_{i=1}^{n} J_i X_i\} \sim -\Delta S/R$, where ΔH, ΔV and ΔS are the enthalpy, volume and entropy effects of the phase reaction, R is the universal gas constant.

Both in natural samples and in plagioclases from our sample, the standard microprobe analysis continuously reveals, besides the main oxides, the presence of FeO, MgO and K_2O in amounts reaching the first percent. Calculation of the stoichiometric composition of the plagioclase converges when Si, Al, Ti, and Fe are involved in the framework motif, hence iron in plagioclases is predominantly in the trivalent form. The compositions of the plagioclases are recalculated into 5 minals - anorthite $CaAl_2Si_2O_8$ (An), albite $NaAlSi_3O_8$ (Ab), orthoclase $KAlSi_3O_8$ (Or), magnoanorthite $MgAl_2Si_2O_8$ (MgAn) and ferrialbite $NaFeSi_3O_8$ (AbFe).

The formation of the above minals from the melt occurs as a result of the following heterophase reactions:

$$CaO^l + 2AlO^l_{1.5} + 2SiO^l_2 = CaAl_2Si_2O_8^{An},$$

$$NaO^l_{0.5} + AlO^l_{1.5} + 3SiO^l_2 = NaAlSi_3O_8^{Ab},$$

$$KO^l_{0.5} + AlO^l_{1.5} + 3SiO^l_2 = KAlSi_3O_8^{Or},$$

$$MgO^l + 2AlO^l_{1.5} + 2SiO^l_2 = MgAl_2Si_2O_8^{MgAn},$$

$$NaO^l_{0.5} + FeO^l_{1.5} + 3SiO^l_2 = NaFeSi_3O_8^{AbFe},$$

Equation (1) implies the form of equations for calculating the minal content of minerals. Example for anorthite minal:

$$X^{An} = \exp\left[\left(A^{An} + \beta^{An}P\right)/T + B^{An} + D^{An}\lg fO_2 + F^{An}W + \sum J_i^{An}X_i + \ln\alpha_{CaO} + 2\ln\alpha_{AlO_{1.5}} + 2\ln\alpha_{SiO_2}\right], \qquad (2)$$

where a_i - the activity of the initial components in the melt according to the two lattice silicate melt model by Nielsen with co-authors (see Frenkel et al., 1988).

Table 1. Values of the coefficients and constants for equations of the form (2) found with the help of the "solver" add-on in the MS Excel program for plagioclase minals.

	An	Ab	Or	MgAn	AbFe
A	3876,00	3396,34	2408,89	12796,3	0
β	-23,4650	49,1090	64,6945	-5,50800	-19,8278
B	2,25955	-6,64126	3,10476	-31,6068	-10,9549
D	0,077001	0,0574623	0,016721	-0,001667	-0,220383
F	0	0	-0,66307	-0,0199	0,171401
J_{Si}	0	7,7329	-9,86244	26,1589	7,19898
J_{Ti}	1,364504	8,3057	-2,277095	23,9169	12,44282
J_{Al}	0	8,8629	0,120355	15,5501	16,23933
J_{Fe}^{3+}	-7,855052	-4,5921	-9,359747	22,3597	6,152822
J_{Fe}^{2+}	3,738744	10,2786	-1,963735	16,2415	5,462782
J_{Mn}	-2,26919	9,0207	-0,9198	19,7139	9,9444
J_{Mg}	0	0,8905	-13,26105	35,0539	10,44178
J_{Ca}	-4,315377	0	1,531609	15,4982	-0,16124
J_{Na}	-3,855258	5,1891	-1,884758	13,6740	-3,080942
J_K	-3,855258	5,1891	-1,884758	13,6740	-3,080942

The corresponding form has expressions for the remaining minals. Finding the coefficients for the variables (optimization) was done by minimizing the squares of the differences between the calculated and experimental minal contents using the "solver" add-on in the MS Excel software (Table 1).

For clarity of comparison of calculated and experimental contents of small elements, calculated concentrations of minals were recalculated by weight percent of oxides. Fig. 2-4 shows the contents of FeO, MgO and K_2O in wt. %.

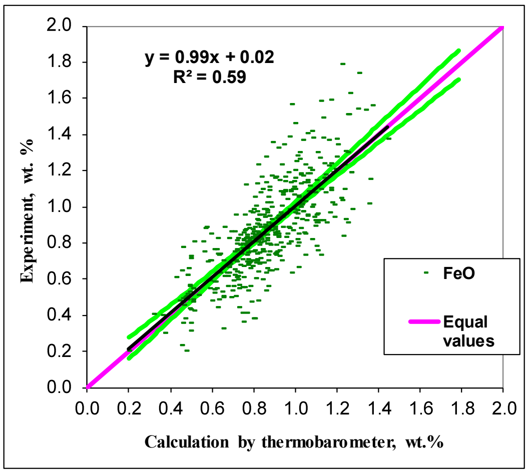

Fig. 2. Comparison of experimental and calculated FeO contents in plagioclases from the sample.

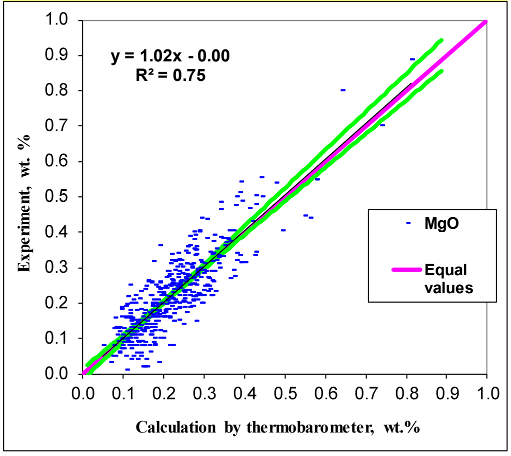

Fig. 3. Comparison of experimental and calculated MgO contents in plagioclases from the sample.

One of the statistically valid criteria for the quality of thermobarometers is the size of the confidence interval at a given level of reliability of the linear regression between the experimental and calculated values. The advantage of confidence intervals for estimating the quality of an equation, in comparison with, for example, standard deviations, is their clarity and the fact that the confidence interval narrows with increasing sample size. On the graphs of Fig. 2-4 boundaries of confidence intervals are indicated by curves of green color.

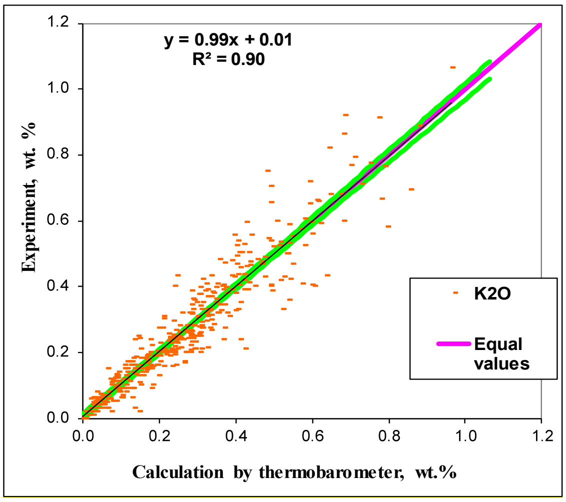

Fig. 4. Comparison of experimental and calculated K_2O contents in plagioclases from the sample.

The error in the prediction of the FeO content does not exceed ± 0.08 wt. % at 95 percent reliability level, MgO – ± 0.04 wt. %, K_2O – ± 0.03 wt. %. This circumstance will allow us to model the fractionation of these elements with a higher accuracy, which may be useful, for example, in procedures of geochemical thermometry.

Acknowledgements. The authors are grateful to AA Ariskin, GS Barmina and GS Nikolaev for their selfless efforts to create and update the INFOREX database.

References:

Ariskin A. A. et al. INFOREX information retrieval system: analysis and processing of experimental data on phase equilibria in igneous rocks //Petrology. – 1997. – vol. 5. – №. 1. – p. 28-36.
Koptev-Dvornikov EV, Bychkov DA Geothermometers for a wide range of compositions of basites: Mat. Conf. "Ultramafite-Mafite Complexes of Pre-Cambrian Folded Regions." Irkutsk. Izd. SB RAS, 2007. P. 178-181.
Frenkel M.Ya., Yaroshevsky AA, Ariskin AA, Barmina GS, Koptev-Dvornikov EV, Kireev BS Dynamics of intra-chamber differentiation of basite magmas. Moscow: Nauka, 1988. 216 c.

Kotelnikov A.R.[1], Korzhinskaya V.S.[1], Kotelnikova Z.A.[2], Suk N.I.[1], Shapovalov Yu.B.[1] Pyrochlore and tantalite solubility in fluoride solutions at T=550-850°C, P=1 kbar in presence of silicate material. UDC 550.8.014

[1]Institute of Experimental Mineralogy RAS, Chernogolovka Moscow district,
[2]Institute of Geology of Ore Deposits, Petrography, Mineralogy, and Geochemistry, RAS, Moscow
(kotelnik@iem.ac.ru, vkor@iem.ac.ru, kotelnik@igem.ru,, sukni@iem.ac.ru)

Abstract. The experimental results of natural pyrochlore and tantalite behavior in KF, NaF solutions in quartz presence at 550-850°C, 1 kbar are presented. A significant effect of the presence of quartz on the solubility of tantalite and pyrochlore in aqueous solutions of alkali metal fluorides under hydrothermal conditions is shown. Investigation of fluid inclusions in quartz shows that in experiment condition the reactions of KF high temperature hydrolysis take place and phase of silicate glass (water solution-melt) forms as a result of interaction with quartz. This phase of alkaline glass is concentrator of Ta and Nb. It has been shown that phase of alkaline solution-melt can be effective concentrator of ore component (Ta, Nb) at last low temperature stages of rare metal granites crystallization.

Keywords: *experiment, pyrochlore ,tantalite, solubility, fluoride solutions, fluid inclusions*

To estimate the influence of silicate matter (or granite melt) on pyrochlore and tantalite solubility in fluoride solutions special runs (with quartz and without it) have been done. The runs lasted 7-15 days at 550°, 650°, 750 and 850°C and pressure 1 kbar in the solutions LiF (0.08 M), NaF (1M); KF (0.5 and 1M) on hydrothermal devices with the external heating and cold valve and in high gas pressure vessel. The accuracy of temperature regulation was ±5°C; pressure ±50 bar. As initial materials quartz (d. Perekatnoye, Aldan), natural pyrochlore of the following composition (recalculation by 4 cations taking charge balance into account): $(Na_{0.92}Ca_{0.95}Sr_{0.06})_{1.93}(Ti_{0.04}Nb_{2.02})_{2.06}O_6[F_{1.02}(OH)_{0.18}]_{1.20}$ and tantalite of the following composition: Ta_2O_5 – 57.50 mas.%; Nb_2O_5 – 25.80 mas.%; MnO – 16.63 mas.%; (formula recalculation by 6 (O): $Mn_{1,03}Nb_{0,85}Ta_{1,14}O_6$) from quartz-amazonite-mica pegmatite of Etyka tantalum deposit have been used. To estimate phase fluid state we used a method of synthetic fluid inclusions in quartz. Quenching solution after the run was analyzed by ICP/MS and ICP/AES (mass-spectral and atomic-emission) method for the elements (Nb,Ta,Na,Ca,Mn,Fe,Ti etc.). Solid charge was analyzed on the electronic microprobe CamScan MV2300 (VGA TS 5130MM) and by the x-ray phase method.

Fluid Phase State Data of fluid phase state have been obtained by a method of synthetic fluid inclusions in quartz. If the fluid at the experiment parameters was homogeneous, all inclusions have the same phase composition and thermobarogeochemical parameters. In the case of a heterogeneous fluid, inclusions of immiscible phases or mechanical mixtures of these phases are captured by different inclusions, resulting in two or more types of inclusions with different thermobarogeochemical characteristics.

The runs with LiF solution (concentration 0.08 M). At pressure 1 kbar and temperatures 550°, 650°C a fluid was in a heterogeneous state: two-phase gas-liquid (G+L) and three-phase gas-liquid-crystal (G-L-C) inclusions occurred in the samples.

The runs with NaF solution (concentration 1M). In contrast to LiF solutions at pressures 0.5 and 1 kbar and temperature 550°C a fluid was in a homogeneous state: only two-phase G-L inclusions were found. At temperature rise up to 650°C the interaction of the fluid with solid phases resulted in precipitation of a small amount of solid phases. The process of homogenization of two-phase inclusions is closely critical what shows the approximation of the run parameters to the critical point of the system.

The runs with KF solution (concentration 0.5-1M). At 550°C and 1 kbar in case of the initial concentration of the solution 2.9 mass% (0.5M) a fluid is homogeneous: only G+L inclusions occur. If at the same P-T conditions the concentration of the initial solution increases up to 1M (5.8 mass %) then a fluid is heterogenized what testifies to the formation of different-type inclusions. So, at conditions studied (550, 650, 750 and 850°C and 1 kbar) 1M solutions of potassium fluoride were heterophase and stratified into a vapor (low concentrated) phase and a phase of the saline fluid.

Pyrochlore and tantalite solubility

It is experimentally determined that at T = 550°C quartz presence decreases essentially Nb content in KF solutions (more than by 3 orders) (fig. 1) (Kotelnikov et al, 2017). For temperatures 650°C and 850°C quartz presence in the system increases the equilibrium content of Nb in the solution by an order of magnitude: at 650°C Nb content in 1M KF without quartz is $2.91*10^{-5}$, but in quartz presence it is $1.59*10^{-4}$ m/ kg H_2O; at 850°C the number of Nb without quartz is $2.38*10^{-4}$, but with quartz (or with granite melt) is $2.39*10^{-3}$ mol/ kg H_2O. The measurement of pH solutions before and after the runs has shown that for 550C the initial solution 1M KF gets alkaline after the run, what decreases pyrochlore solubility; for 650°C pH shifts into the acidic region but only by half an order of magnitude; for 850°C pH after the run shifts into the acidic region markedly: (pH bef/exp. =7.32, but pH aft/exp. = 1.901). It has been suggested that by means of fluid-magmatic interaction at T=850°C HF concentration in fluid essentially increases.

Figure 2 shows the temperature dependence of the equilibrium tantalum (Fig. 2a) and niobium (Fig. 2b) content during dissolution of tantalite in 1M KF and 1M NaF, depending on the presence of quartz (granite melt).

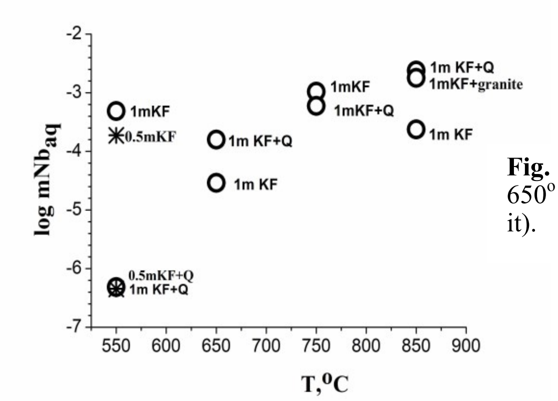

Fig. 1. Pyrochlore solubility in the solutions 0.5 and 1M KF at 550°, 650° and 850°C and P = 1 kbar (in the presence of quartz and without it).

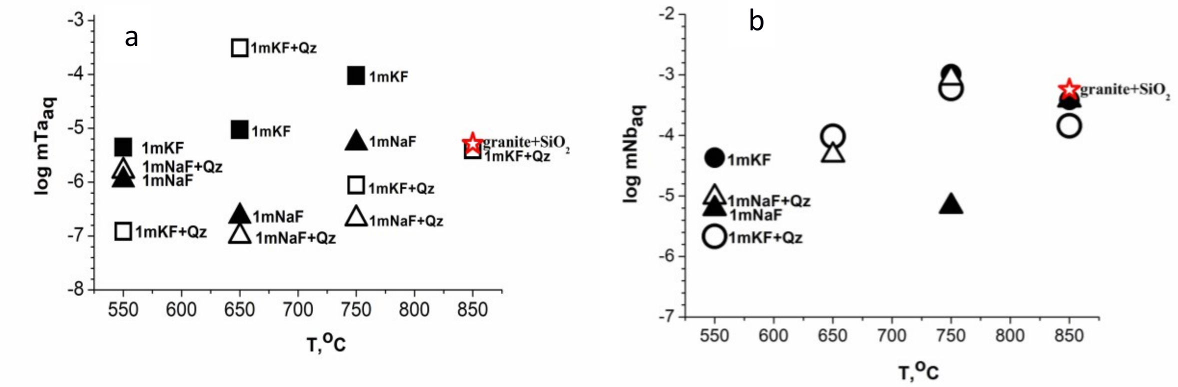

Fig, 2. Temperature dependence of the equilibrium tantalum (a) and niobium (b) content upon dissolution of tantalite in 1M KF and 1M NaF, depending on the presence of quartz (granite melt). a – painted shapes – without quartz; not painted – with quartz; star – granite + quartz.

Table 1. Phase compositions in the runs of pyrochlore and tantalite solubility in presence of silicate phase.

Oxide	850°C, 1kbar, 1M KF (Mcl+Qz+granite)			850°C, 1kbar, 1M KF (Pchl+Qz+ granite)			650°C, 1kbar, 1M KF (Pchl+Qz)	
	Mcl	Tnt	Granite glass	Pchl	Granite glass	Rippite	Pchl	Sil. glass
F	4.06	-	1.86	5.41	3.02	-	4.82	0.98
Na_2O	5.43	-	1.58	7.66	2.81	-	7.55	0.36
Al_2O_3	-	-	9.63	-	10.13	-	-	-

Oxide	850°C, 1kbar, 1M KF (Mcl+Qz+granite)			850°C, 1kbar, 1M KF (Pchl+Qz+ granite)			650°C, 1kbar, 1M KF (Pchl+Qz)	
	Mcl	Tnt	Granite glass	Pchl	Granite glass	Rippite	Pchl	Sil. glass
SiO_2	-	-	52.37	-	55.18	38.90	-	71.35
K_2O	0.80	-	14.19	-	15.53	15.93	1.2	10.69
CaO	8.76	-	0.16	13.84	0.87	-	15.28	-
MnO	1.16	15.08	2.07	1.26	-	-	0.40	0.26
Nb_2O_5	7.14	18.63	3.59	69.94	6.02	45.52	72.11	8.16
Ta_2O_5	73.15	66.11	6.11	-	-	-	-	-
Sum	100.70	99.82	91.56	99.21	93.56	-	101.36	91.80

Notice. Mcl – microlite, Tnt – tantalite, Pchl – pyrochlore, Sil. glass – silicate glass.

The investigation of fluid inclusions in quartz has shown that under the conditions of the runs the reactions of high-temperature hydrolysis KF take place: $KF + H_2O = KOH\downarrow + HF\uparrow$; here the interaction with quartz takes place: $SiO_2 + 2KOH = K_2SiO_3 + H_2O$, with the formation of silicate glass phase (aqueous solution-melt). This phase of alkaline glass is a concentrator of Ta and Nb (tabl. 1). Tantalum and niobium contents (Ta_2O_5 and Nb_2O_5) in granite melts reach 6 mas.% (850°C). When pyrochlore is dissolved in 1M KF (650°C) in the presence of quartz, a silicate melt with Nb_2O_5 content of up to 8 wt.% is formed.

Thus, the phase of the alkaline silicate solution-melt can serve as an effective concentrator of the ore component (Nb and Ta) at the last low-temperature stages of crystallization of rare-metal granites. Fig. 3 shows the comparison of the data of the niobium content in 1M KF solution in the presence of quartz for the natural minerals pyrochlore and tantalite. As can be seen, the dependences of the contents of niobium in the solution are of the same type.

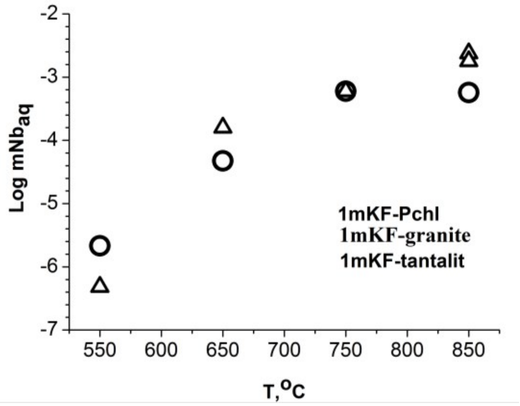

Fig, 3. Comparison of the data of the niobium content in 1M KF solution in the presence of quartz for the natural minerals pyrochlore (triangles) and tantalite (circles).

Based on the results obtained, it is possible to outline the scheme of the granite melt evolution with a decrease in the TP parameters. The following stages of the process of oreogenesis of fluoride granites with Nb-Ta type of mineralization can be distinguished:

1) T=900°C; P=4 kbar. Raising a homogeneous silicate melt enriched with F, K, Nb with a fluid in the sub-saturated state. Ore elements are present in the melt.

2) T=900→800°C; P=4→2.5 kbar. Separation of a part of the fluid from the melt ("retrograde boiling"); the separating fluid at such TP-parameters is homogeneous. The ore elements (Nb, Ta) are predominantly concentrated in the melt (relative to the fluid). The beginning of crystallization of the main rock-forming minerals; depending on the composition of the melt, this may be quartz, or feldspar, or nepheline. The residual melt and fluid are enriched with incoherent components (F, Nb, H_2O, etc.). A fluid containing KF undergoes hydrolysis according to the scheme: $KF + H_2O \rightarrow HF \uparrow + KOH$. In this case, according to D.S. Korzhinskiy (1982) rule, the alkaline component is distributed into the melt, and acid (HF) - enriches the fluid phase.

3) T = 800 → 700 ° C; P = 2.5 → 1 kbar.

Crystallization of both rock-forming and ore minerals (pyrochlore crystallizes under fluid redundancy conditions). There is a heterogenization of the fluid to the vapor and liquid phases. In this case, the liquid phase of the fluid sharply enriches with alkaline components (Na, K), as well as by such main elements as Si and Al, according to the reactions: $KF + H_2O \rightarrow HF \uparrow + KOH$; $2KOH + SiO_2 \rightarrow K_2SiO_3 + H_2O$ ("heavy fluid"). In this case, a highly alkaline solution-melt is formed, which interacts with the residual melt, forming a single solution-melt (Korotaev, Kravchuk, 1985). This highly alkaline solution-melt concentrates the ore elements, that is, there is an accumulation of ore elements in the residual melt phase. This melt can be wrung out along the cracks from the bulk of the crystallizing intrusion.

4) T = ≤ 700 ° C; P = ≤1 kbar. Complete crystallization of the intrusion (including the highly alkaline silicate phase of the residual solution-melt). Under the action of the residual fluid, the alkaline elements (Na, K) are removed and the ore minerals (pyrochlore, rippite) are crystallized from the residual solution-melt.

This study was supported by RFBR, project № 15-05-03393-a.

References:

Korzhinskiy D.S. The theory of metasomatic zoning. M: Nauka, 1982. 104 p.
Korotaev M.Yu., Kravchuk K.G. Heterophasicity of hydrothermal solutions under conditions of endogenous mineral formation. Preprint. Chernogolovka. 1985. 62 p,
Kotelnikov A.R., Korzhinskaya V.S., Kotelnikova Z.A., Suk N.I. Pyrochlore solubility in fluoride solutions at 550-850°C, P=1 kbar in presence of silicate material**.** In: Proceeding of Russian Annual Seminar of Experimental Mineralogy, Petrology and Geochemistry (RASEMPG-2017), Moscow, April 18-19, 2017. P. 124-127.

Shubin I.I.[1,2], Zharkova E.V.[2], Koptev-Dvornikov E.V.[1]. Senin V.G.[2]. Oxygen fugacity in the formation of Kiwakk intrusive: results of simulation and experimental measurements. UDC 550.843 (543.559)

[1] M.V. Lomonosov Moscow State University, Department of Geology, Moscow,
[2] V.I. Vernadsky Institute of Geochemistry and Analytical Chemistry RAS, Moscow (shubin.ivann@mail.ru).

Abstract. The Kivakka intrusion is located in North Karelia on the north-western shore of the Piaozero Lake. For the experiment, pure grains of olivines (Ol), orthopyroxenes (Opx) and clinopyroxens (Cpx) were selected. The determination of the intrinsic oxygen fugacity (fO_2) of minerals were carried out on a high-temperature furnace based on two solid electrolytes in the temperature range from 800 to 1100 ° C. We found out good agreement between the experimental and the model data (KOMAGMAT).

Keywords: *intrinsic oxygen fugacity; minerals; Kivakka intrusion; model; experiment.*

The Kivakka mafite-ultramafic intrusion is part of the Olang group of stratified peridotite-gabbro-noritic intrusives belonging to the sublatitudinal band of basite-hyperbasite massifs. This intrusion is located on the north-western shore of Lake Piaozero in North Karelia. The enclosing rocks are represented by migmatized biotite and amphibole gneisses, granite gneisses and granodiortogneisses of the upper Archean [Bychkova, Koptev-Dvornikov 2004].

The intrusion is an originally overturned cone with a calculated height of the axis of 3.9 km and an angle at the apex of 80 degrees [Khvorov et al. 2000; Koptev-Dvornikov et al. 2001]. At the present position, the axis has a slope of 36 degrees to the northwest. The upper 2000 meters of the cut are exposed by erosion, which allows us to judge its inner structure and rhythmicity [Bychkova, Koptev-Dvornikov 2004]. The scheme of the intrusion is shown in Fig.1.

In the structure of the Kivakka intrusion, several zones can be distinguished according to the mineral composition: lower contact, olivine, noritic, gabbro-noritic, and gabbro-noritic with pigeonite, upper contact. Bottom-up the section there is a transition to the stratified series through interlacing with the reverse order of the replacement of cumulative parageneses (from gabbro-norites to olivinites). Preliminary explore of the thin sections, chose those rocks in which the least number of secondary minerals. Mono fractions of olivines (Ol), orthopyroxenes (Opx) and clinopyroxenes (Cpx) from the rocks of the supporting vertical section of the intrusion, which have been least subjected to various secondary changes, such as serpentinization, were selected for the experimental determination of the intrinsic oxygen fugacity. For measurements samples were taken from near contact zone (KV 401 Opx), olivinites zone (KV 410 Ol), from a small area of perelivania bronzite and harzburgites in the upper part olivinites zone (KV 419 OPx), a small bronzite zone (KV 421 Opx), norite zone (KV 420 Ol, OPx and OPx KV 438), gabbro- noritic zone (SQ 457 Opx, Cpx KV 467, KV 467 Opx), gabbro-norite with pigeonite (KV 475 Opx).

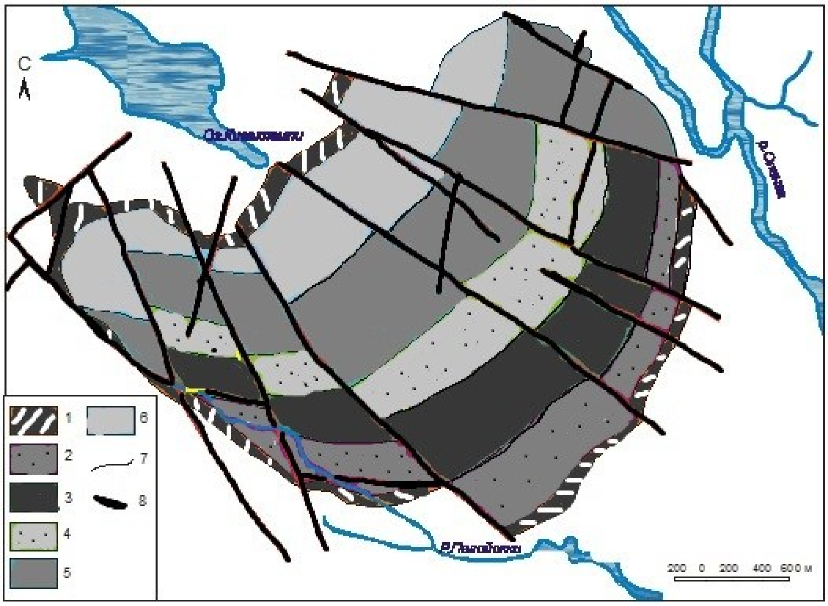

Fig.1. The structure of the Kivakka intrusion (version of Y.V. Bychkova). Legend: 1-Lower and Upper Contact zone (LCZ and UCZ); 2-Olivinite zone (OZ); 3,4-Noritic zone (NZ) (3-subzone of interbedding of the Bronzites and Norits (SzIBN)); 5-Gabbro-noritic Zone (GNZ); 6-Zone of Gabbro-norites with pigeonite (ZGNp); 7-geological boundaries; 8-discontinuous violations.

The determination of the intrinsic oxygen fugacity of the mafic minerals was carried out on a high-temperature unit based on two solid electrolytes in the temperature range from 800^{0}C to 1050^{0}C at a pressure of 1 atm [Zharkova, 1989]. The temperature measurement accuracy was ±2^{0}C, the intrinsic oxygen fugacity ± 0.2 lg fO_2 [Zharkova E.V. 1989]. . The results of the experiments are given in Table 1.

The results of measurements of the intrinsic oxygen fugacity of minerals were compared with the calculated fO_2 data obtained using the COMAGMAT program [Ariskin, Barmina 2000] (Table 1) (Koptev-Dvornikov, oral report). The contents of the normative rock-forming minerals in the studied samples [Koptev-Dvornikov et al., 2001], the measured values of fO_2 and intrinsic oxygen fugacity of Ol, Opx and Cpx, obtained in the realistic model of the formation of the Kivakka intrusion are given in Table 2.

Experimental data of the intrinsic oxygen fugacity of minerals are compared with the parameters of the realistic model of the Kivakka intrusion (KOMAGMAT-3.5) [Frenkel et al., 1988] with a different Fe $^{+2}$ fraction from 0.99 to 0.97 of total iron in the original magma. The most accurate measurements are consistent with the model with an iron ratio of 0.97. The original magma contained 25% of intralelluric olivine crystals and 75% of the melt (simulation results). The rocks deviated from the model at the base of the section, in the direction of increasing oxygen fugacity, in which a different fraction of intrathelluric olivine was present. A near-linear empirical dependence of oxygen fugacity on the proportion in the intrathelluric olivine rock for the lower part of the intrusive section is established (Fig. 2). The measured fO_2 in minerals from rocks in which intathelluric olivine is absent is in good agreement with the model.

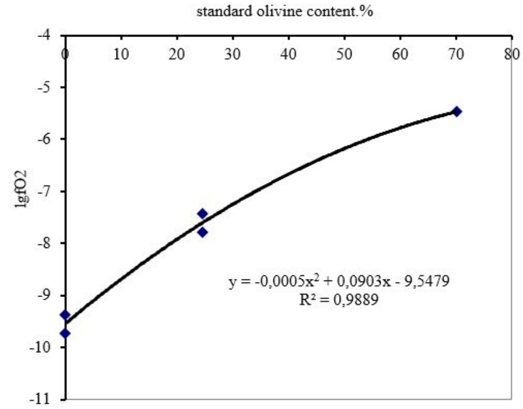

Fig.2. Graph of the dependence of oxygen fugacity on the content of intrathelluric olivine in the rock in the lower part of the intrusive section.

Table 1. Values of coefficients "A" and "B" for empirical dependencies lg $fO2 = A + B / T^oK$ for various minerals of the Kivakka intrusion.

Sample	A	B	r	n
KB-401 OPx	18,8	-40221	0,998	7
KB-410 Ol	32,9	-57979	0,986	7
KB-419 OPx	12,5	-33286	0,980	7
KB-419 CPx	14,4	-35612	0,974	7
KB-420 Ol	23,8	-46858	0,975	7
KB-420 OPx	22,3	-45025	0,989	7
KB-421 OPx	24,5	-48027	0,998	7
KB-438 OPx	13,1	-34195	0,992	7
KB-457 OPx	19,3	-41769	0,994	7
KB-467 OPx	18,4	-40367	0,989	7
KB-467 CPx	23,9	-47865	0,987	7
KB-475 OPx	25,2	-48524	0,992	7

r - coefficient of correlation, n - number of experimental points.

Table 2. Normative content of Cpx, Opx and Ol in the rock; experimental and calculated datas of fO_2 for minerals of the Kivakka mafic-ultramafic intrusion

№ sample	Cpx	Opx	Ol	lgfO_2 exp	lgfO_2 mod	T °C mod	lgfO_2- lg$fO_{2\ QFM}$
KB 401 Opx	3,1	28	0	-7	-9,5	1280	+0,35
KB 410 Ol	3,4	14,8	70,2	-5,5	-9,7	1237	+2,32
KB 419 Opx	14,9	25,3	0	-9,7	-9,6	1223	-1,71
KB 419 CPx	14,9	25,3	0	-9,4	-9,6	1223	-0,51
KB 420 Ol	4,4	50,9	24,6	-7,4	-9,6	1223	+0,58
KB 420 Opx	4,4	50,9	24,6	-7,8	-9,6	1223	+0,18
KB-421 Opx	5	75,9	5,1	-7,5	-9,6	1223	+0,48
KB 438 Opx	7,2	32,4	0	-9,9	-9,5	1211	-1,71
KB-457 Opx	18,5	24,5	0	-9,1	-9,3	1194	-0,78
KB-467 Opx	18,4	19	0	-9,3	-8,9	1180	-0,81
KB-467 Cpx	18,4	19	0	-9	-8,9	1180	-0,51
KB-475 Opx	19,1	18,6	0	-8,4	-8,4	1167	+0,24

Conclusions:

1) In the lower ultramafic part of the section, the polynomial dependence of lg fO_2 on the content in the intrathelluric olivine rock was established.
2) For rocks whose minerals were formed in the intrusion chamber (does not contain intratelluric olivine), the experimental data do not contradict the parameters of the realistic model of the formation of the Kivakka intrusion (COMAGMAT 3.5).

References:

Ariskin A.A, Barmina G.S. Modeling of phase balance in the crystallization of basaltic magmas. - Moscow: Nauka, MAIK "Nauka / Interperiodica", 2000. - 363 p.

Bychkova Ya. V., Koptev-Dvornikov E.V. Rhythmic stratification of the Kivakka type: geology, petrography, petrochemistry, the hypothesis of formation. Petrology. 2004. T. 12, No. 3. P. 281-302.

Zharkova E.V. Determination of oxidation-reduction conditions for the formation of minerals of peridotite rocks of the upper mantle by the method of electrochemical oxygen cells. Sc.w. for the competition. of a sc. d. of PhD. chem. sciences, Moscow, 1989.

Koptev-Dvornikov E.V., Kireev B.S., Pchelintseva N.F., Khvorov D.M. Distribution of cumulative parageneses, rock-forming and secondary elements in the vertical section of the Kivakka intrusion (Olang group of intrusives, North Karelia). Petrology, 2001, Vol. 9, No. 1, pp. 3-27.

Khvorov D.M., Koptev-Dvornikov E.V., Bychkova Ya. V. Reconstruction of the form of the Kivakka layered intrusion, "Petrography at the Turn of the 21st Century, Results and Prospects", II All-Russian Petrographic Meeting, Syktyvkar, 2000. - P. 224-227.

Frenkel M.Ya., Yaroshevsky A.A., Ariskin A.A., Barmina G.S., Koptev-Dvornikov E.V., Kireev B.S. Dynamics of intra-chamber differentiation of basite magmas. Moscow: Nauka, 1988.

Suk N.I.[1], Kotelnikov A.R.[1], Peretyazhko I.S.[2], Savina E.A.[2]. Evolution of trachyrhyolite melts based on experimental data. UDC 550.89:553.21

[1]Institute of Experimental Mineralogy RAS, Chernogolovka Moscow district,
[2]A.P. Vinogradov Institute of Geochemistry SB RAS, Irkutsk (sukni@iem.ac.ru, kotelnik@iem.ac.ru, elen_savina@mail.ru)

Abstract. Experimental study of melting of trachyrhyolites with different F contents was produced in high gas pressure vessel in presence of H_2O or H_2O_2 at different regimes: 1) at T=1250°C and P=5.5 kbar during of 6 h; 2) melting at T=1250°C and P=5.5 kbar (duration of 2 h) and then parameters were reduced to T=900°C and P=1 kbar (duration of 4 days); 3) T=950°C, P=4 kbar (duration of 6 h) => T=750°C, P=1 kbar (duration of 5 days); 4) T=950°C, P=4 kbar (duration of 6 h) => T=650°C, P=1 kbar (duration of 5 days). At T=1250°C and P=5.5 kbar immiscible splitting into aluminosilicate and fluoride-calcium melts was observed when F content in the system was ≥5 wt%. Study of REE (La, Ce, Y, Gd, Dy) distribution between immiscible phases shows that REE predominantly concentrate in fluoride melt.

Keywords: *experiment, melt, liquid immiscibility, trachyrhyolite, partition coefficients, effusive rocks*

It has been investigated melting of trachyrhyolites discovered among effusive rocks of Nilginsky depression in Central Mongolia and belong to dzunbainsky suite of early Cretaceous. In trachyrhyolites of one of overtrusts the rocks anomaly enriched in Ca and F were discovered. In these rocks content of CaO and F run to 15-20 and 10-15 wt % respectively. To study trachyrhyolites of three types were selected. They differ in F content (0.58, 2.45 and 15.0 wt %). These rocks are presented by light-gray or light-lilac porphyric rocks with phenocrysts of quartz and feldspars (sanidine). Mineral composition of selected rocks is identical and differs only in fluorite content.

Experimental method

Experiments were produced in high gas pressure vessel in different regimes. In first series melting was produced at T=1250°C and P=5.5 kbar during of 6 h in presence of 10 wt% H_2O.

Second series of experiments was produced in conditions imitated volcanic process i.e. in decrease of temperature and pressure which is typical for the process of the magma rise to the earth surface.

Experiments were produced in three regimes: 1) T=1250°C, P=5.5 kbar (duration of 2 h) and then parameters were reduced to T=900°C, P=1 kbar (duration of 4 days) in presence of 10 wt% H_2O; 2) T=950°C, P=4 kbar (duration of 6 h) => T=750°C, P=1 kbar (duration of 5 days) in presence of 10 wt% H_2O_2 solution; 3) T=950°C, P=4 kbar (duration of 6 h) => T=650°C, P=1 kbar (duration of 5 days) in presence of 10 wt% H_2O_2 solution. Then isobaric quenching was produced. The trachyrhyolites of Central Mongolia of three types with different F content (0.58, 2.45 and 15 wt%) or mixtures of trachyrhyolites with minimal and maximal F content in proportions 1:1, 2:1 and 1:2 were used as starting materials.

Experiments to study phase distribution of REE have been produced at T=1250°C and P=5.5 kbar during of 6 h with addition of REE (La, Ce, Y, Gd, Dy) oxides (1 mg for each). The experimental samples were analyzed on a digital scanning electron Tescan Vega II XMU microscope.

Experimental data At T=1250°C and P=5.5 kbar in the sample with maximum F content (15 wt %) it has been obtained liquid immiscibility between silicate and fluoride-calcium melts, which produce drops of one liquid in another (fig. 1). Trachyrhyolites with F content of 0.58 and 2.45 wt % were melted forming homogeneous glass. In sample obtained during trachyrhyolite with 0.58 wt % F melting the quenching crystals of calcium fluoride were observed. Average compositions of phases obtained are presented in table 1.

Table 1. Compositions of phases obtained during trachyrhyolite melting at T=1250°C and P=5.5 kbar.

Oxides, wt.%	7060[1]	7061		7062	Element, wt.%	7060
		glass	total[2]			
	n=7	n=4	n=4	n=12		n=7
SiO_2	70.57	70.70	65.09	72.62	Si	4.17
Al_2O_3	10.43	10.52	9.86	10.79	Al	0.73
Na_2O	2.92	2.92	2.80	3.10	Na	0.07
K_2O	5.79	5.19	4.94	5.33	K	0.67
CaO	0.15	0.95	4.71	0.58	Ca	44.83
FeO	0.65	0.76	0.36	0.42	Fe	0.00
F	1.59	0.31	2.61	0.42	F	35.53
Sum	92.10	91.35	90.37	93.26	O	14.00
∑ O=2F	91.43	91.22	89.27	93.08	Sum	100

[1] Samples numbers obtained during trachyrhyolite melting: 7060 – 15 wt.% F, 7061 – 2.45 wt.% F, 7062 – 0.58 wt.% F.

[2] total – total glass composition with quenching crystals of calcium fluoride.

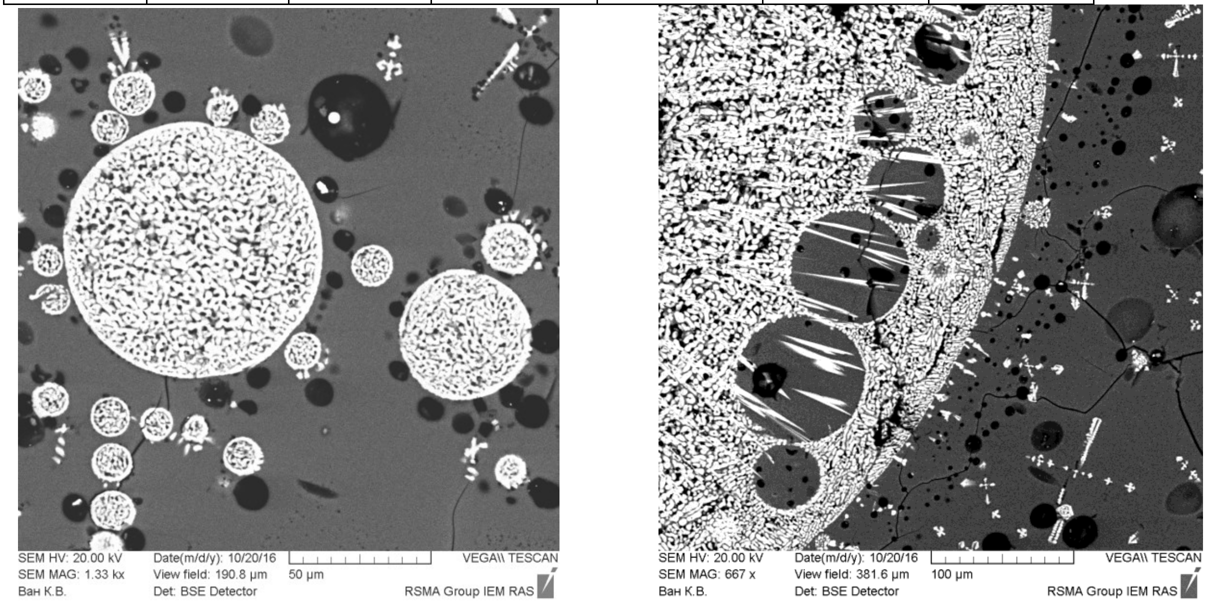

a **b**

Fig. 1. Liquid immiscibility between silicate (dark) and fluoride-calcium (light) melts, obtained at T=1250°C and P=5.5 kbar. BSE image.

Second series to study trachyrhyolite melting was produced in conditions imitated volcanic process i.e. in decrease of temperature and pressure which is typical for the process of the magma rise to the earth surface and its eruption.

In the sample of trachyrhyolite with maximum F content produced in regime T=1250°C, P=5.5 kbar => T=900°C, P=1 kbar liquid immiscibility between silicate and fluoride-calcium melts appeared too, but smaller isometric, roundish and dumbbell shape segregations are observed (fig. 2) which approached experimental samples to natural trachyrhyolite image. Compositions of fluoride-calcium phases reply to fluorite composition. Fluorite crystals probably formed during quenching were observed, too.

In the sample with 2.45 wt.% F content some small roundish and dumbbell shape segregations of fluoride-calcium phase were observed. It evidences that when TP-parameters decrease immiscible field expand and compositions of coexisting phases become more contrast.

In the trachyrhyolite sample with maximum F content obtained in regime T=950°C, P=4 kbar (duration of 6 h) => T=750°C, P=1 kbar (duration of 5 days) in presence of 10 wt% H_2O_2 solution both roundish and dumbbell shape segregations of fluoride-calcium phase and segregations without evident roundish form are observed (fig.3). Formed fluorite crystals are presented, too. It is likely to evident about beginning of fluorite forming at these parameters. Probably field of coexisting of silicate, fluoride-calcium melts and fluoride crystals takes place.

In the trachyrhyolite sample with maximum F content obtained in regime T=950°C, P=4 kbar (duration of 6 h) => T=650°C, P=1 kbar (duration of 5 days) in presence of 10 wt% H_2O_2 fluorite forming is likely to happen. Its segregations have not evident roundish form but look like fluorite grains in silicate matrix (fig. 4). Sometimes crystals of dark-colored mineral (perhaps pyroxene) occur.

To estimate the minimum F concentration when liquid immiscibility can arise in the system the experiments with mixtures of trachyrhyolites with minimum and maximum F contents in ratio 1:1, 2:1 and 1:2 have been produced at T=1250°C and P=5.5 kbar. Calculated F contents in the samples studied were 7.27, 5.15 and 9.40 wt % approximately. In all experiments liquid immiscibility was obtained. But in the sample with 5.15 wt % F content minimum amount of drops of fluoride-calcium phase was observed. These data show that liquid immiscibility can arise when the system contain F content >5 wt %.

Investigation of REE (La, Ce, Y, Gd, Dy) distribution between layered phases at T=1250°C and P=5.5 kbar showed that they predominantly concentrate in fluoride melt (tabl. 2).

Petrographical observations and data of study of melting inclusions in minerals from trachyrhyolites evidence about coexistence of trachyrhyolite (aluminosilicate) and fluoride-calcium melts as at the stage of mineral phenocrysts growth in magma chamber so at lava eruption. This fact is proved out by our experimental investigations.

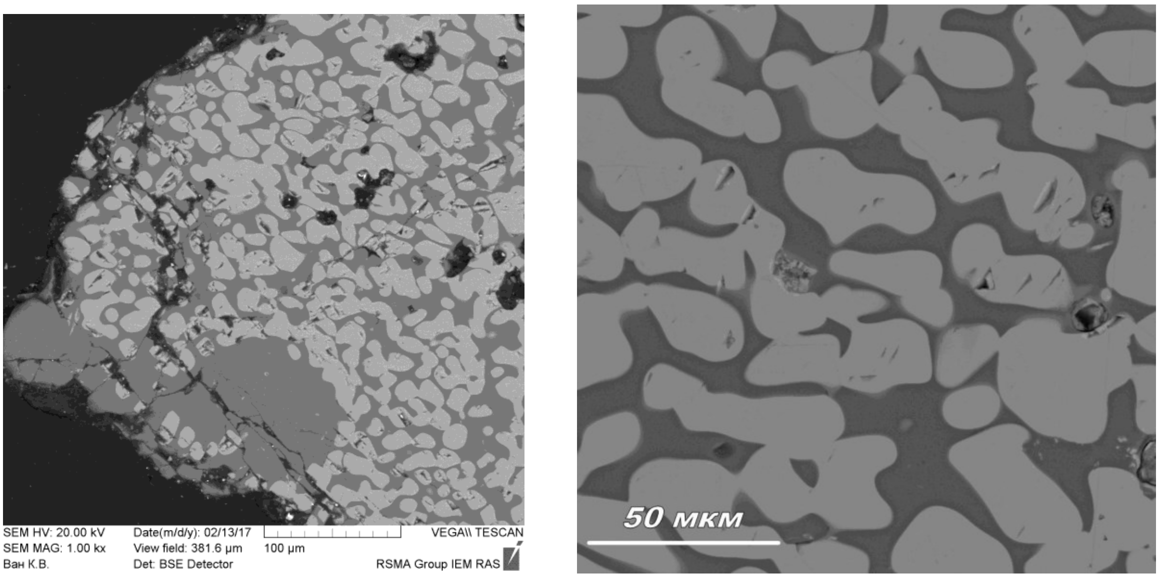

Fig. 2. Liquid immiscibility between silicate (dark) and fluoride-calcium (light) melts, obtained in conditions with decrease of temperature and pressure (T=1250°C, P=5.5 kbar => T=900°C, P=1 kbar). BSE image.

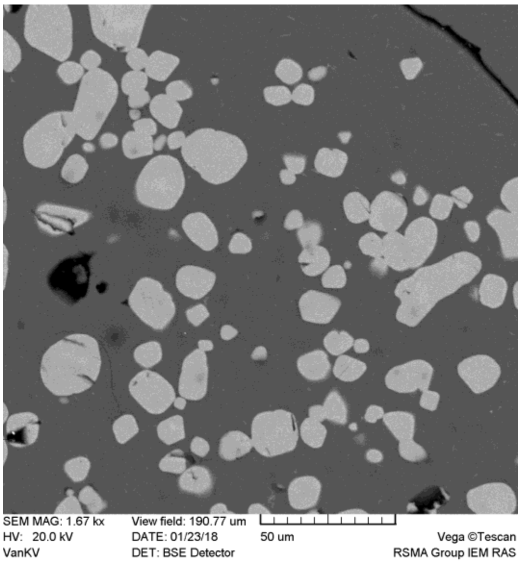

Fig. 3. Phases (silicate – dark and fluoride-calcium – light) obtained in conditions with decrease of temperature and pressure (T=950°C, P=4 kbar => T=750°C, P=1 kbar). BSE image.

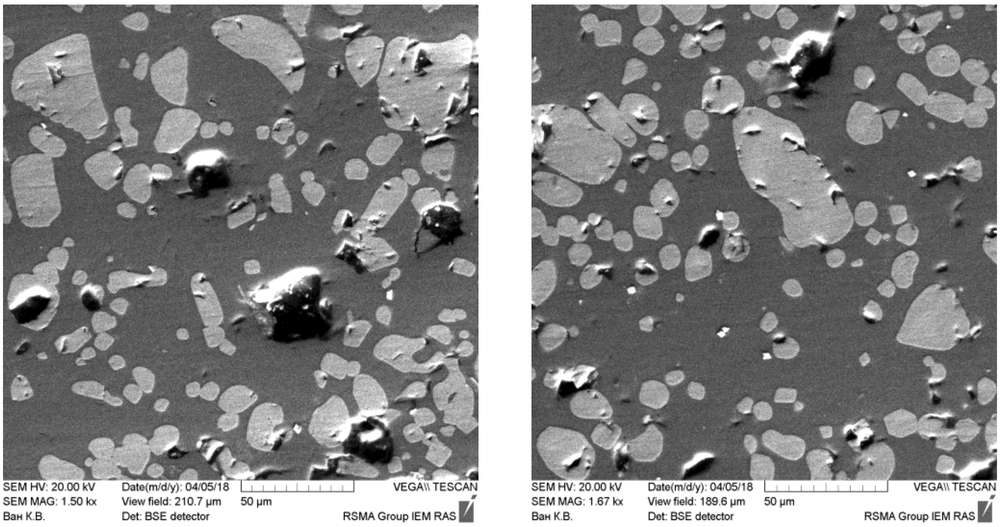

Fig. 4. Phases (silicate – dark and fluoride-calcium – light) obtained in conditions with decrease of temperature and pressure (T=950°C, P=4 kbar => T=650°C, P=1 kbar). BSE image.

Table 2. Compositions of phases obtained during trachyrhyolite mixtures melting at T=1250°C and P=5.5 kbar.

Oxides, wt.%	RIO-1[1]	RIO-2	RIO-3	Element, wt.%	RIO-1	RIO-2
	n=6	n=4	n=3		n=3	n=6
SiO_2	63.96	65.52	62.28	Si	8.33	8.96
Al_2O_3	9.73	10.06	9.25	Al	0.96	1.01
Na_2O	2.21	2.30	1.48	Na	0.40	0.39
K_2O	5.09	4.51	3.95	K	0.94	0.81
CaO	1.15	1.04	3.21	Ca	27.94	28.25
FeO	0.48	0.71	0.50	Fe	0.00	0.00
Y_2O_3	0.16	0.05	0.39	Y	3.79	2.88
La_2O_3	0.24	0.07	0.17	La	2.62	1.70
Ce_2O_3	0.28	0.25	0.52	Ce	4.08	3.55
Gd_2O_3	0.28	0.23	0.24	Gd	3.08	5.40
Dy_2O_3	0.12	0.26	0.23	Dy	3.03	4.04
F	0.37	0.41	0.53	F	29.80	23.28
Sum	84.07	85.41	82.76	O	15.03	19.73
∑ O=2F	83.91	85.24	82.54	Sum	100	100

[1] Mixtures of trachyrhyolites with minimum and maximum F contents in ratio 1:1 (RIO-1), 2:1 (RIO-2) and 1:2 (RIO-3).